Modeling Thermal Behavior of Vehicle Integrated Photovoltaics

Thesis

Presented in Fulfillment of the Requirements for the Undergraduate Honors Research Distinction in the College of Mechanical Engineering at The Ohio State University

By

Kellen McCabe

The Ohio State University

2021

Thesis Committee

Ardeshir Contractor, Advisor

Clarissa Belloni

Abstract

With a changing environment and a massive push toward clean energy and sustainable practices, technological advancements of electric vehicles (EV) are an important step to improve as a society in this area. A current downside of EVs is their limited driving range. With recent developments in photovoltaic (PV) materials and manufacturing technologies and declining PV costs, the integration of PV cells into vehicle exterior bodies as an added power source has become an emerging research area. Unlike conventional PV module installations on roof-tops and power plants, in the case of vehicle integrated photovoltaics (VIPV), PV cells are directly integrated into vehicle body with no convective cooling on the underside. The integrated module can only dissipate heat from the top side, experiencing higher temperatures. Limiting cell temperatures is important as the conversion efficiency of PV cells decreases with increasing temperatures. To maximize VIPV system efficiency and investigate long term structural integrity, understanding the effects of parameters such as drive cycle, location, season, and PV material on module temperature and thereby PV efficiency is key. In this study, the effect of these parameters is investigated using numerical modeling. First a geometric model of a simplified VIPV module was created. To mimic the environmental conditions of an integrated module, representative thermal, electrical, and structural boundary conditions were defined. Using the generated model and boundary condition definitions, governing equations for heat

transfer and structural mechanics were solved using the finite element software COMSOL Multiphysics. A systematic study was conducted to isolate the effect of each parameter on module temperature and performance. Though this study, temperatures and resulting thermal stresses of vehicle integrated modules is quantified. Estimating these stressors will help guide module design for high energy yield and service life.

Acknowledgments

This undergraduate thesis was made possible because of guidance and assistance from Navni Verma, who meet and advised on a weekly basis. In addition, the oversight and guidance from advisor Prof. Ardeshir Contractor was crucial to the study. I would also like to acknowledge both the Smart Vehicle Concept Center as the project sponsor and Prof. Clarissa Belloni who participated in the defense committee for this thesis.

Vita

My name is Kellen McCabe, I am from the Cleveland area and I am completing my final year of undergraduate studies in Mechanical Engineering. I have experience working internships with a company related to utilities at Davey Resource Group. Recently I have accepted a job working for Epic, a healthcare solutions software company based out of Madison, Wisconsin. Personally, I am very thankful for the opportunities and experience this project has provided me. With goals to work in an environmentally conscious field, work with electric vehicles and photovoltaic cells was a great experience to have during my undergraduate studies.

Table of Contents

List of Tables

List of Figures

Chapter 1. Introduction

1.1 Electric Vehicles and Limitations

As we look to overcome our carbon emissions as a global society, electric vehicles, or EVs, have become a core focus of the push to green alternatives. Visualized by Figure 1, EVs have been growing every year in the global automotive market share but have still have not made the big break into the market that many have hoped. This could be due to some key limitations in the functionality of EVs, most specifically: driving range.

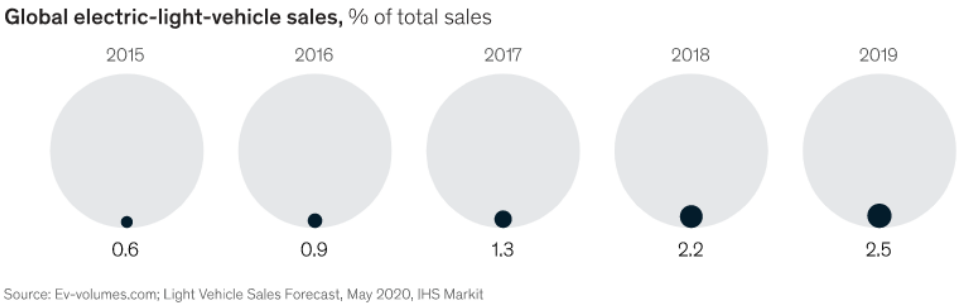

Figure 1: Market Share Trend of Electric Vehicles (Gersdorf et al., 2020)

There are multiple means to improve the range of EVs, from increasing battery capacities to finding ways to decrease load. Falling into the second of the categories is vehicle integrated photovoltaics (VIPV). VIPV simply, is integrating photovoltaic cells into the exterior surface of vehicles. As an application this means it can take on a lot of shapes and form, as it can be integrated into the roof, sides, and hood of a car for example. The integrated PV module may be connected to the vehicle's primary or auxiliary batteries

or both for gains in range extension or battery sizing. VIPV provides a promising option as an additional source for charging these vehicles. Vehicles may charge while driving or while being parked in a parking lot which may reduce charging times and charging intervals.

1.2 Photovoltaic Costs

Cost is a key factor in VIPV application, as the integrated module must be cheap enough that it does not significantly increase vehicle price, but instead adds inherent value with its power producing potential. As the costs of PV technology decreases year after year, the price is nearing ranges that make PV integration in vehicles favorable. Figure 2 shows the trend of the cost per watt for multi-crystalline silicon PV modules from 2008 to the end of 2018, highlighting a drop to just above 5% of the initial value in 2008 (Green, 2019). This trend has pushed PV technology into a much more affordable range VIPV applications, and with more breakthroughs with the material and manufacturing technology, this price will continue to trend downward in the future.

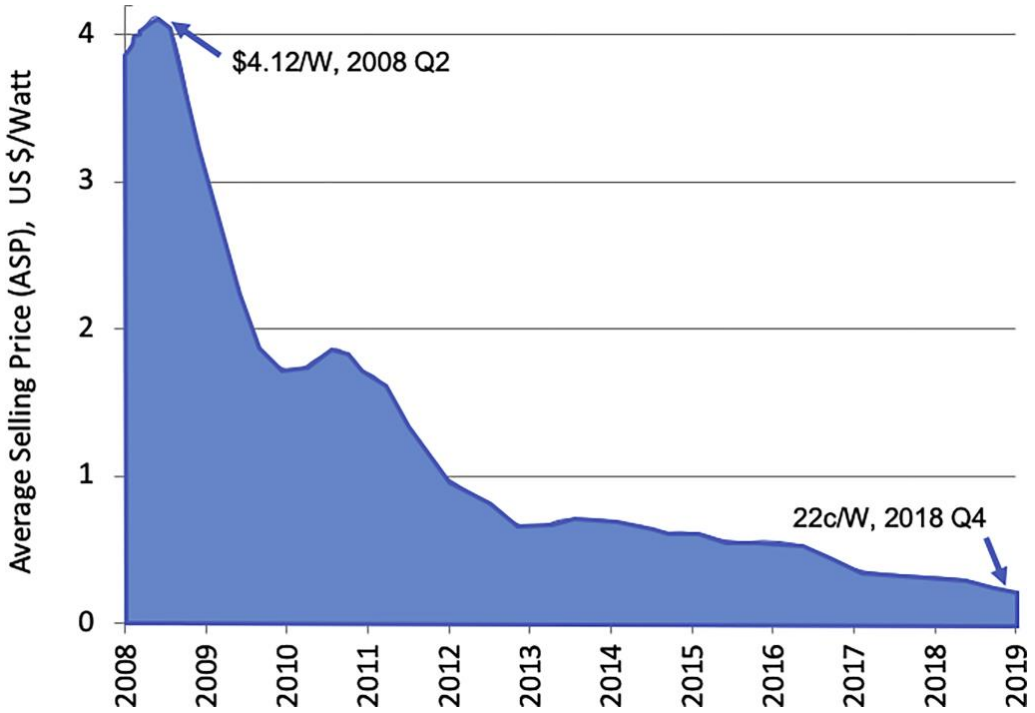

Figure 2: Price Trend of PV over the Past Decade (Green, 2019)

As prices decreases, the scope of possible PV applications grows drastically. With applications similar to VIPV, a limiting design factor is size and to best take advantage of a limited space, higher efficiency cells are more desirable but add to the cost of the module. Adding an extremely expensive PV module to the relatively limited roof size of a vehicle for it to be exposed to high temperatures and many other factors that limit the effectiveness of the application makes no sense, as the gained charging power would not outweigh the initial cost and possible repair costs to such an expensive part of the vehicle. With these prices trending down, especially for the high efficiency PV materials, these opportunities become very viable and are a way to directly add value to EVs for a relatively lower investment.

1.3 Vehicle Integrated Photovoltaics

Currently the research and design of VIPV is surging within automotive companies as they search for the future of development for EVs. Chasing this technology are manufacturers such as Hyundai (Hyundai, 2021), Sono Motors (Sono Motors, 2016), Lightyear (Lightyear, 2021) and Hanergy (Hanergy, 2021), who are working with Alta Devices, to develop this technology. These companies are all making strides in the realm of commercial VIPV applications, looking at the aesthetics as well as power producing potential. Figures 3 and 4 show Fraunhofer ISE's concept vehicle and Hyundai design for VIPV panels in a commercial application.

Figure 3: Example of the Fraunhofer VIPV Concept (Fraunhofer, 2021)

Figure 4: Example of the Hyundai VIPV Concept (Hyundai, 2021)

At the forefront of the future of this technology is Toyota, working with SHARP (Toyota Motor Corporation, 2019) to integrate PV into the current Prius and understand the possibilities high-efficiency solar have in this application. Figure 5 shows the completed prototype of the collaboration between these two companies.

Figure 5: Example of the Toyota VIPV Concept (Toyota Motor Corporation, 2019)

Although it may not be the most pleasing to the eye, this design incorporates the triple-junction compound solar cell modules with efficiencies nearing 34% to both the hood and roof of the vehicle, increasing the overall area. Compared to the previous rendition of this VIPV Prius, the approximate power output for the newest demo car is over 450% greater, giving a massive increase in added driving distance from 6 km to nearly 45 km. The work done by Toyota and SHARP is a great indication to the future of high efficiency cells in the VIPV and how it could impact the VIPV market.

Even though companies like Toyota are advancing this technology, VIPV is still an extremely new technology and there is a lot more to learn about it. In VIPV modules, far less heat will be dissipated from the module as there is no cooling from the backside of the panel, that typical PV modules experience in power plant or roof-top applications. Losing

less heat means the panel is going to reach high temperatures. Understanding effects of these elevated temperatures on the module and how this affects performance and degradation of modules is critical.

1.5 Design Challenges

The design process of VIPV gains more challenges due to the extremely limited area available for the design. When compared to typical applications, area is a far lower concerning factor, meaning minor losses in efficiency are usually acceptable but not favorable. In VIPV, the efficiency must be maintained to a higher standard because of the much more limited area. In addition, the high temperatures that VIPV experience add to the concern of the design because of the relationship between cell temperature and PV efficiency. In Figure 6, we see a trend showing the decrease in overall power of PV cells as the temperature increases. The effect of temperature is different for each material and is best captured using the temperature coefficients of these materials.

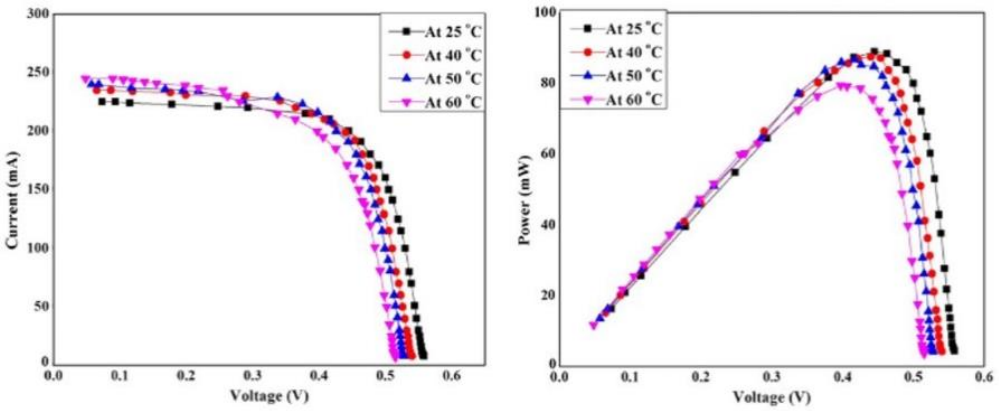

Figure 6: IV and PV plots with Varying Temperatures (Chander et al., 2015)

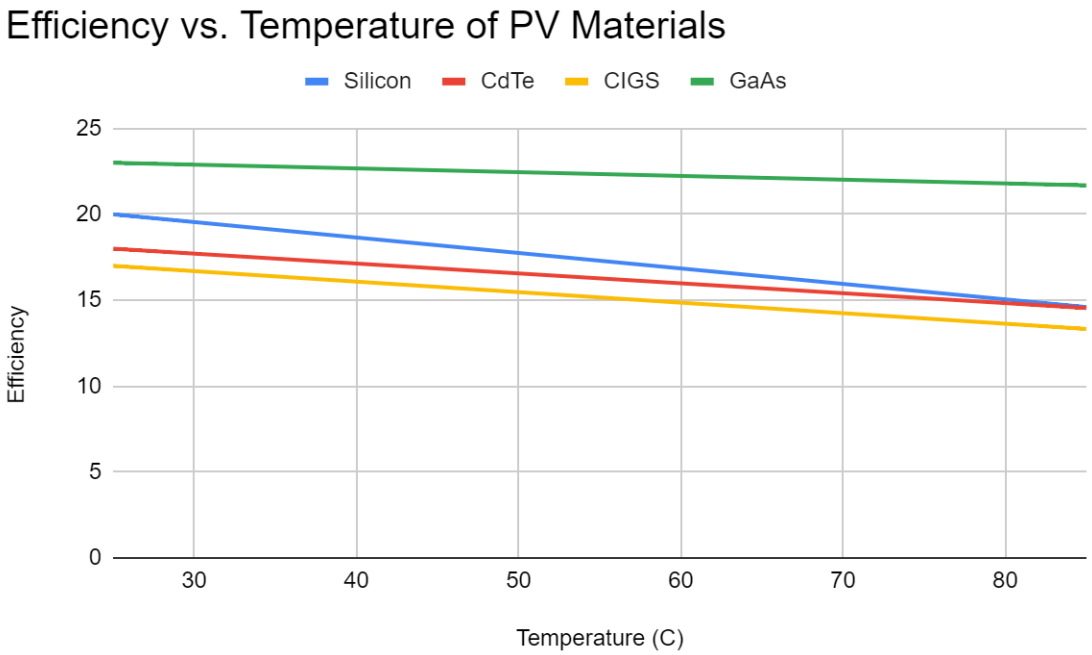

Figure 7: Efficiency vs Temperature of Selected Materials

In Figure 7, the linear relationship for different PV materials efficiency when compared to temperature is provided. Differences in slope and initial values are apparent and are the reasons that some PV materials are more applicable to higher temperature environments. This linear relationship between temperature and efficiency is defined by the temperature coefficient.

Looking at the effects of temperature on the VIPV design process, we must first understand that VIPV is a high temperature application. With the module integrated directly to the vehicle roof, no air is flowing across the backside of the panel, whereas typical PV applications will see losses from this side of the module. This indicates that the temperatures could be higher in VIPV because we are losing energy from less surface area of the module. As mentioned before, higher temperature for the PV cells translates to a

lower efficiency, which directly decreases our overall performance. Either limiting the temperature of these cells or the effects of higher temperature on these cells is extremely important as a decrease in efficiency can cause more of the irradiation to be converted to heat, thus decreasing the efficiency further in a vicious cycle.

Limitation of temperature or its effects is key moving through every aspect of VIPV design including the packaging materials and the cell layout in the module. With different cell layouts available such as shingled or thin film, these designs react differently to temperatures and handle the stresses and possible degradation that come with the thermal cycling. The module must be robust enough to account for the thermal stresses and degradation due to thermal cycling that are associated with these temperatures in a PV application. These stresses lead to the delamination of layers of material in the module. This is due to thermal mismatch caused by different expansion rates of the different module materials at higher temperatures and repeated thermal cycling, materials within a VIPV module are susceptible to delamination, which is a major reason for studying the thermal response of VIPV modules to guide design process. Table 1 shows the different thermal expansion coefficients and the difference in these values is the cause for the delamination that occurs and causes degradation.

Table 1: Thermal Expansion Coefficients

Material	Thermal Expansion Coefficient (α)
Ethyl Vinyl Acetate (EVA)	90e-6 K^{-1}
Silicon	2.6160e-6 K^{-1}
Steel	22e-6 K^{-1}

In addition, VIPV extends the understood “triad” of key properties of PV from efficiency, cost, and reliability by adding in both specific power and for more commercial

considerations, aesthetics of the final design. Instead of only being concerned with these original aspects of the design, the specific power, which address the power output per weight is focused on limiting the added load on the battery by the module. Challenges come in VIPV with PV cell layouts or materials that have a high mass associated with the area that the design is being applied to. In EVs, any additional mass is direct load being added to the vehicles drive system and in the case of VIPV design, any mass in the VIPV is working directly against the power output of the module. In Figure 8 we see a comparison of areal density of different complete PV modules and notably we see the differences in mass added when comparing some thin film PV modules like CdTe and CIGS versus the heavier c-Si designs.

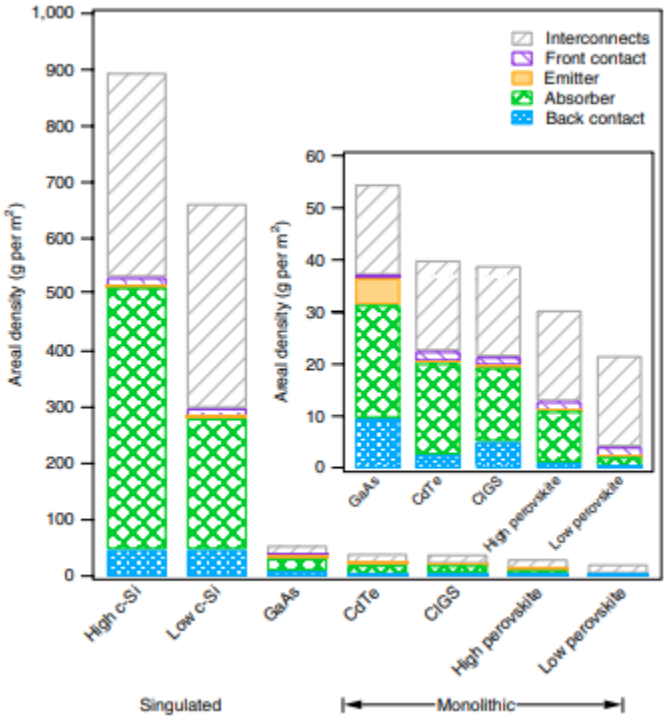

Figure 8: Areal Density of PV Materials and Packaging Methods (Reese et al., 2018)

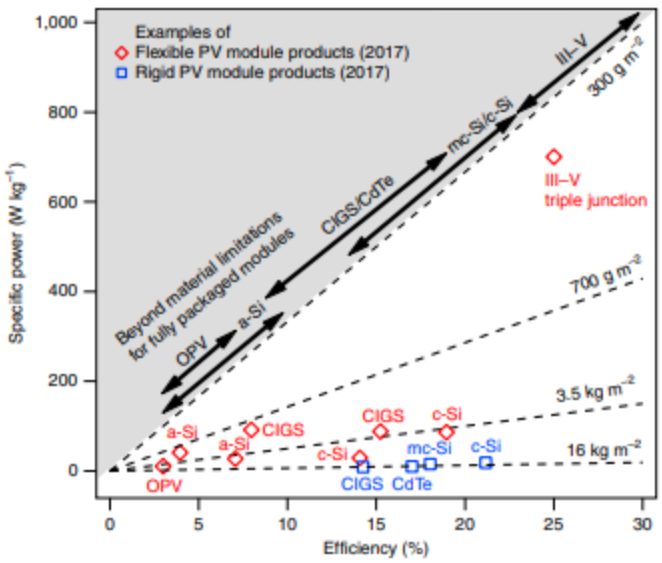

Figure 9: Specific Power and Efficiency of PV materials (Reese et al., 2018)

In Figure 9 we see a comparison of different specific powers and efficiencies of typical PV modules products. Notably, the III-V triple junction materials are far ahead of the competition in this regard and have a very high wattage for each unit of mass added to the system. This would result in more direct value in a VIPV design because we are adding little load to the drive system of the EV. The need to maximize the specific power of these panels is why all aspects of the PV module being integrated are important. The materials and design aspects used to fix the PV cells and interconnections is a huge factor in this, as some may be lighter while some may be less prone to delamination and stress damages mentioned above.

Finally, the aesthetics of the design are important as the appearance of cars is greatly valued in the market. Finding a way to smoothly integrate the PV cells into the vehicle's appearance could vastly improve the value people consider it adds. This design challenge is best encompassed by the development of the coatings and glass alternatives

that are being explored as a top layer for VIPV modules. Coatings need to strike a balance between transmitting enough light through to the cells while also appearing pleasing on the vehicle. Most importantly, many vehicles can be parked outside and exposed to both harsh winter and hot summers and must stand the functional test of time, not wearing or losing the mechanical integrity that is desired.

Taking in all these challenges, VIPV has a lot to overcome to best fill this role in improving the possibilities of EVs. The designer must strike a balance between finding limitations in temperature effects as well as a light weight and visually appealing design, but most importantly, always make decisions to maximize the efficiency of the design. Moving forward, the study of VIPV and the high temperatures of the modules will help further understand the constraints for the design. Getting indication for the temperatures within VIPV will help understand what coatings, packaging methods, and PV technologies are best for this application.

1.6 Motivation

A comprehensive numerical model would allow for better insight into the thermal and mechanical challenges in the design of VIPV system. The importance of thermal effects in VIPV is high as it has a direct relationship to metrics that determine the viability of VIPV in a space constrained energy system. This model will allow for the comparison between different PV materials, looking at the efficiency and stress results, indicating which PV materials are suited for this application. Additionally, the model can also serve to help design effective thermal management solutions to address these challenges. The

modeling framework developed in this study can also be extended to study thermal behavior of building integrated photovoltaics, in which case the heat transfer constraints on the system are similar.

This work is part of a project sponsored by Smart Vehicle Concepts Center (SVC) at OSU. The sponsored project involves developing a research tool that serves as virtual platform to analyze performance of VIPV systems for different vehicle formats and drive cycle applications. The analytical model currently does not account for the temperature dependent efficiency of PV materials while calculating PV output. The contributions of the present study will result in more accurate predictions of gains and help elucidate technical merits of VIPV.

1.7 Objectives

The objective of this study is to develop a multi-physics, three-dimensional numerical model to predict the thermal, mechanical and electrical performance of vehicle integrated photovoltaics for various environmental conditions. The specific objectives of this thesis are as follows:

1. Create three-dimensional geometry of vehicle roof with integrated photovoltaic module.
2. Model thermal transport for roof integrated PV including heat conduction through all module layers, convective heat loss to external flowing air and radiative heat loss to ambient to predict 3D temperature distribution of module.
3. Couple the thermal and mechanical models to predict stress and strain distribution.

4. Develop electrical model to predict PV output using predicted thermal response as input.

5. Using the coupled thermal-mechanical-electrical modeling framework developed, conduct a systematic study of effects of parameters such as solar irradiation, ambient temperature, wind speed, vehicle formats, PV materials, and others on the overall system performance.

6. Prepare the model as a framework to be applied to future studies and technologies.

Chapter 2. Materials and Methods

2.1 Literature Review

In the past study of PV applications and modeling the thermal and stress responses, numerical modeling has been a key tool to understand effects of different parameters, allowing for cheap simulations compared to true prototyping alternatives. Most commonly, we see these models in the PV plant and roof top PV fields. Although there are many similarities with the PV applications modeled in the past and VIPV, key differences in the heat loss on the module obstructs these models from translating. While the end application may be different, studying the process these studies have performed will give insight on assumptions and decisions that can be made in the numerical analysis.

There are several studies that have been previously conducted to model the thermo-mechanical response of modules. In Singapore, researchers modelled a PV module mono-Si showing the relationship temperature has with stresses and efficiency considering an environment with convective and radiation losses of heat from the module using FEM. They found losses of 3% efficiency when temperature rose 40 °C (Lee & Tay, 2012b). In another study, researchers compared silicon panels with and without a cooling heat exchanger using modeling and simulation and found that cooling has a can maintain efficiency at around 3% higher when compared to an uncooled module after the module experiences a 50 C increase in temperature. To validate their model, they made comparisons using experimental data from Florida Solar Energy Center (Usama Siddiqui et al., 2012). In a similar study, researchers used computation fluid dynamics to analyze the performance of an actively cooled PV module utilizing a thermal collector with mono-

Si found that the radiation cooling is key to difference in losses between an uncooled panel and the actively cooled panel (Siddiqui & Arif, 2013). Although all these models thoroughly cover the intricacies of the multi-physics withing the PV system, they lack key connections to this projects model due to the different boundary conditions of VIPV.

More can be taken away from these articles on the front of assumptions and boundary condition applications. All these studies chose to model the convective losses using a convective coefficient rather than completely modeling the air around the module as a simplifying assumption. In addition, based on a control volume analysis solar cells are typically modeled as volumetric heat sources. From the incident radiation, a fraction (8 %) of energy is reflected, fraction (based on cell efficiency) is converted to electricity and the remaining is dissipated as heat. Although some of these studies chose to assume that the heat losses from the free convection on the panel are too minor to model, this was ignored as VIPV has scenarios with the car at a complete stop and the forced convection is null in this condition (Arora, 2016; Lee & Tay, 2012a; Nižetić et al., 2016; Nyanor, 2015; Siddiqui & Arif, 2013; Usama Siddiqui et al., 2012).

2.2 Model Development

2.2.1 Governing Equations:

Detailed in Figure 10 is the overall heat transfer occurring throughout the module. Irradiance from the sun comes into the panel, depending on the location, season, and time of day. This is an input into the heat source equation, which is modeled as a volumetric heat source from the PV cells in the module. The heat source all depends on the

efficiency of the cells which depends on the current temperatures of the cells. There are heat losses occurring on the top side of the panel in the form of radiative losses and convective losses. The radiative losses depend only on material properties as well as the current module temperature and the ambient temperature. The convective losses are dependent on velocity of the air as well as the current temperature of cells and the ambient temperature.

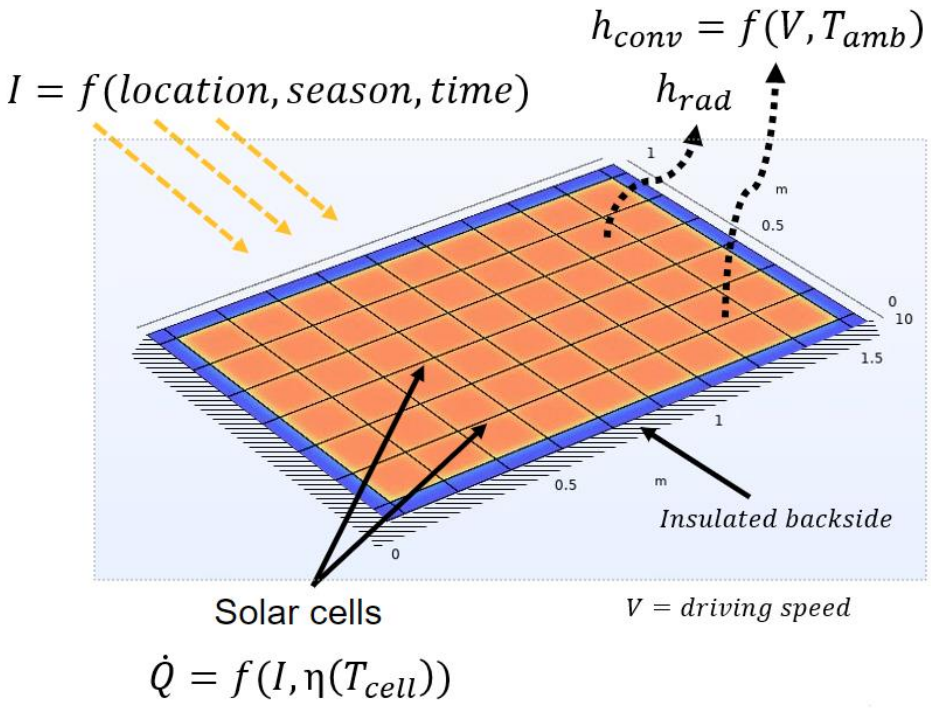

Figure 10: Heat transfer overview of module

Solving for thermal transport in the module involves solution of the conservation of energy equation. In its most general form, this equation is listed below.

Equation 1: $$q_{in} - P_{out} - q_{loss} - C_{mod}\frac{dT_{mod}}{dt} = 0$$

Where q_{in} represents the power added to the system as heat from the solar energy hitting the module. P_{out} represents the power produced by the PV cells in the system with

$C_{mod}\frac{dT_{mod}}{dt}$ representing the thermal lumped capacitance of the system. The q_{loss} term represents a summative loss flux term that can be broken down in Equation 2 where q_{rad} and q_{conv} are values calculated later.

Equation 2: $$q_{loss} = q_{rad} + q_{conv}$$

Summarizing the heat transfer fluxes in this problem with Equation 1, we first see heat fluxes within the model of conduction, through the different material layers. These are the only directional fluxes that occur within the geometry of our system. For heat losses due to both radiative cooling and convective cooling, these are applied as boundary conditions to the outermost surface of the model. As for heat entering the system, the energy that reaches our PV cells that is not converted to power is converted to thermal heat, so the heat entering the system is modeled entering through the cells. The energy reaching our PV cells in the insolation that hits the top of the module minus 8% that is reflected through the glass or top coating layer of the module. Outside of the fluxes occurring in the model, the heat is also stored within the panel using the heat capacities of the materials in the layers.

First, the heat source is calculated using Equation 3.

Equation 3: $$q_{in} = (1 - \eta\ ) * I_{sol}$$

Where η represents the cell efficiency (%) of the VIPV module and I_{sol} (W/m^2) represents the radiative energy from the sun that reaches the PV cells.

Cell efficiency is calculated using Equation 4

Equation 4: $$\eta = \eta_{ref} * (1 - \beta_{ref}(T_{cell} - T_{ref}))$$

Where T_{cell} is the current temperature of the cell while T_{ref} refers to the temperature used when finding the refence efficiency and is often standard testing conditions (STC) of a temperature of 25 deg C. β_{ref} is the temperature coefficient found from testing while η_{ref} is the efficiency of the cell at T_{ref}.

From Equation 3, it is seen that the heat generated is a function of insolation, efficiency, and the area of the cells. As mentioned previously, cell efficiency is also dependent on the temperature of the cells, and as that temperature increases, lower fraction of the insolation is converted to power and higher fraction is lost as heat. This aspect of the problem is where the heating of the cells really compounds on itself and can create bigger problems. The insolation involved in the heating source equation is a function of multiple parameters including location, season, and time of day. The variability for these parameters, especially for a vehicle are cause for the different levels of thermal cycling a VIPV module can experience.

Next, the heat loss by radiation to ambient is calculated using Equation 5

Equation 5: $$q_{rad} = \varepsilon\sigma A(T^4 - T_{amb}^4)$$

where ε represents the emissivity of cells. For this study, the emissivity value was assumed to be 0.92. σ represents Boltzmann's constant, a value used in radiative calculations. A represents the surface area of the top of the module. As mentioned previously T and T_{amb} represent the surface temperature and ambient temperature, respectively. Equation 5 is only dependent on the temperature of both the surface of the module as well as the ambient temperature. Similar to insolation, ambient temperature is dependent location, season, and time of day.

Finally, convective heat losses are calculated using the following equations for forced, free and combined convective cooling. First, the Nusselt number for a forced convection represented by Nu_{forced} is calculated using Equation 6.

$$\text{Equation 6:} \quad Nu_{forced} = 0.680\, Re_L^{1/2} Pr^{1/3}$$

Where Re represents the Reynolds number and Pr represents the Prandtl number. These values are found using Equation 7 and Equation 8.

$$\text{Equation 7:} \quad Re = \frac{uL}{\nu}$$

$$\text{Equation 8:} \quad \text{Pr} = \frac{\nu c_p}{k}$$

In Equation 7, u represents the wind speed, which in this study is synonymous with car speed, while L represents the characteristic length of the module and ν represents the dynamic viscosity of the air. In Equation 8, c_p represents the specific heat of the air with k representing the thermal conductivity of the air. The free convection Nusselt number (Nu_{free}) is calculated using Equation 9.

$$\text{Equation 9:} \quad Nu_{free} = 0.54\, Ra_L^{1/4}$$

Where Ra represents the Rayleigh number and can be calculated using Equation 10.

$$\text{Equation 10:} \quad Ra = \frac{g\,\beta\,(T - T_{amb})L^3}{\nu\alpha}$$

In Equation 10, g represents the acceleration due to gravity, β represents the thermal expansion coefficient, assumed to be 1/T for simplification. T represents the surface temperature of the module while T_{amb} represents the ambient temperature of the air. L represents the characteristic length as mentioned before with α representing the thermal diffusivity. The Nusselt numbers are then combined using Equation 11.

Equation 11: $Nu_{total}^3 \approx Nu_{free}^3 + Nu_{forced}^3$

With Nu_{total} representing the combined effective Nusselt number that is in turn used to calculate the effective convective coefficient (h) in Equation 12.

Equation 12: $h = \frac{Nu_{total}k}{L}$

The calculated h value is then in turn used to calculate the final convective heat loss in Equation 13.

Equation 13: $q_{conv} = hA(T - T_{amb})$

With the A representing the exposed surface area of the module as described in the calculation of radiative losses.

The convective losses are centered around the assumption that the boundary layer formed on the module surface is turbulent. Convective heat loss is dependent on the cooling by the airflow around the module which can be considered using the convective coefficient. The forced convective coefficient depends on the velocity of the air as well as its turbulence while the free convective coefficient depends on the orientation of the flat plate. Overall, the function for total convective cooling depends on the surface and ambient temperature as well as velocity of the air around the module. Equation 1 and Equations 4-12 (were sourced from Fundamentals of Heat and Mass Transfer (Bergman et al., 2015).

2.2.2 Geometry Generation

To begin the development of the model, the three-dimensional module geometry was created in COMSOL, making decisions on the thicknesses and sizing of the different layer within the module. Constraints for overall size of the module were first considered.

Looking at EVs and the applicable space on the roof, an overall area of ~1.5 m^2 was selected with a width of 1.0628 m and length of 1.52 m. Then, silicon cells of 156x156 mm were fit into an array within that over area, using 2 mm gaps between the cells. The thickness of the silicon wafers in the model is 0.18 mm. These wafers are then incased in a layer of ethylene vinyl acetate (EVA) both above and below them, with an overall thickness of 0.98 mm that extends past the edges of the cell array with a small margin to complete the area. The sheet metal used in the manufacturing of cars has a thickness of 0.7 mm, so a layer of sheet steel with this thickness is placed at the bottom of the geometry to represent the car roof. A final image of the geometry can be seen below in Figure 11.

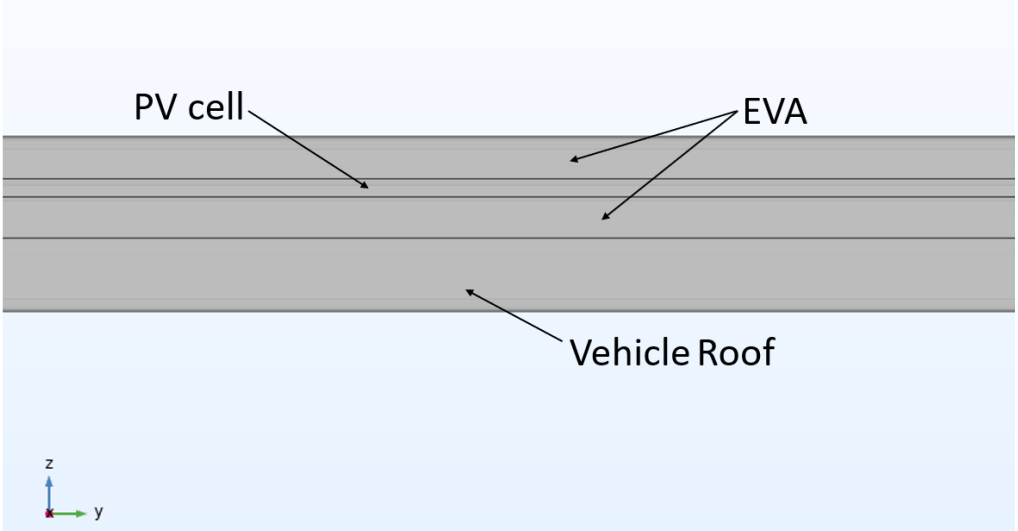

Figure 11: Geometry Cross-section

2.2.3 Material Properties

The thermo-physical properties of the different layers of the VIPV module are included in Table 2 (Bergman et al., 2015).

Table 2: Module Material Properties

Material	Thickness (mm)	Heat Capacity (J/(kg*K))	Density (kg/m^3)	Thermal Conductivity (W/(m*K))
Silicon, mono	0.18	677	2330	130
Sheet Steel	0.7	903	2702	237
EVA	0.98	2090	950	0.311

Table 3: Air Properties for Convective Calculations

Prandtl Number	0.707
K (W/(m*K))	26.3 e-3
Rho (kg/m^3)	1.1614
Alpha (m^2/s)	22.5 e-6
Viscosity (m^2/s)	15.89 e-6

Table 3 lists the thermo-physical properties of air found using (Bergman et al., 2015), with a value of the film temperature at 340 K using Equation 14. These values were then used to calculate convective cooling losses.

Equation 14: $T_{film} = \frac{T_{surf}+T_{amb}}{2}$

Table 4: Efficiency vs Temperature of PV Materials

Material	Reference Efficiency (%)	Temperature Coefficient (%/C)	Reference Temperature (deg C)
Si	20	0.45	25
CdTe	18	0.32	25
CIGS	17	0.36	25
GaAs	23	0.095	25

Looking at different possible PV materials, the differences in their temperature coefficient as well as their STC efficiency are key to their possible success in VIPV. In Table 4, these values are listed for multiple materials based on module information provided by suppliers including First Solar (FirstSolar, 2020) for CdTe, MiaSole (MiaSole, 2017) for CIGS, and Alta Devices (Alta Devices, 2014) for GaAs.

Drive Cycles

Drive cycles used as an input into the model in the form of vehicle velocity were gathered with assistance from the NREL drive cycle tool (NREL, 2021). To cover a range of cycles, the ones selected were city, suburb, and highway drive cycles that had variation in the frequency of stops as well as in the average speed of the vehicle. Figure 12 is an example of a drive cycle used, with a speed vs time trend for the vehicle. For the simulation, this speed factor was input as wind speed for the convective cooling of the module in Equation 7.

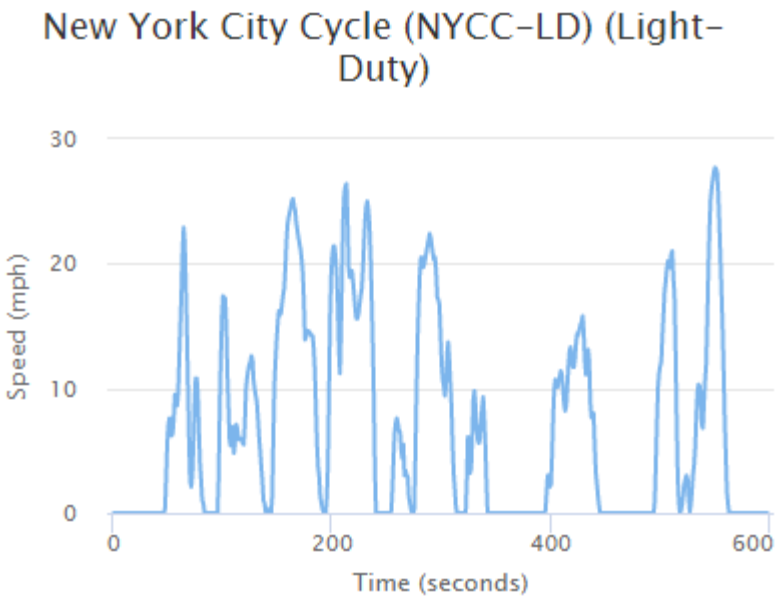

Figure 12: City Drive Cycle (NREL, 2021)

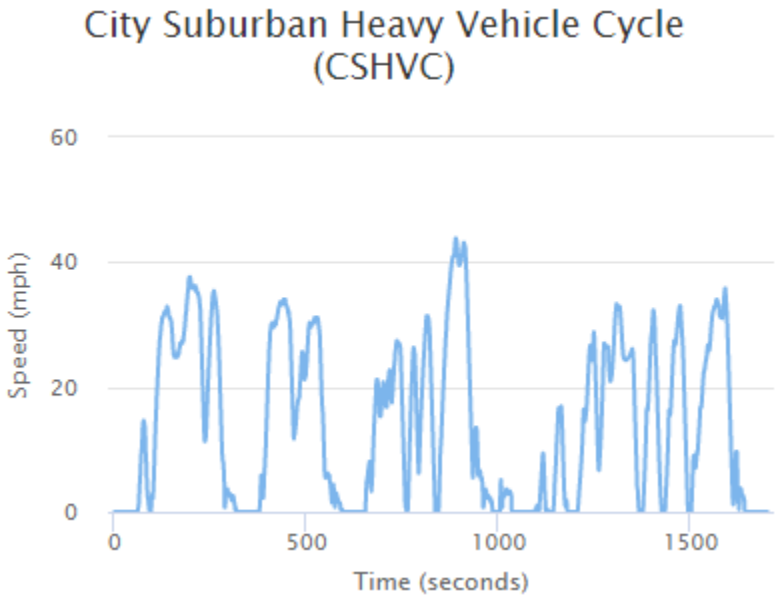

Figure 13: Suburban Drive Cycle (NREL, 2021)

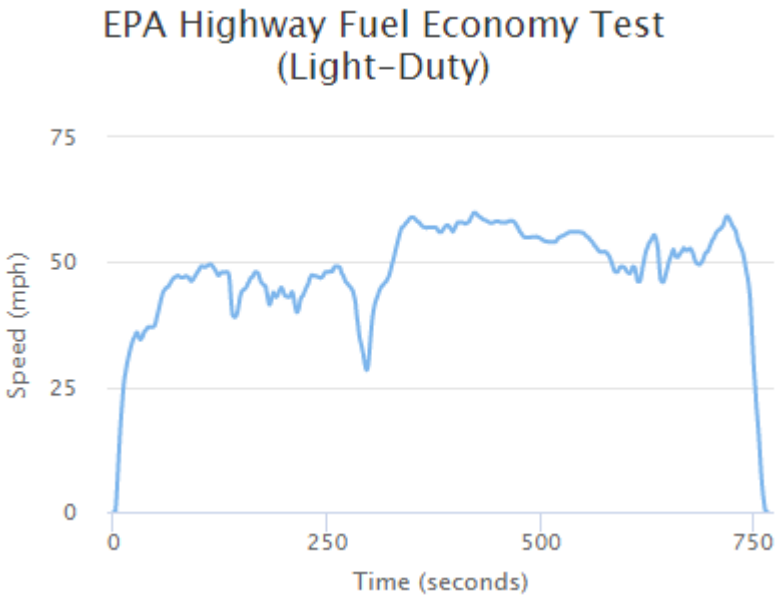

Figure 14: Highway Drive Cycle (NREL, 2021)

2.2.4 Meshing

With the completed geometry the next step to the completion of the model is the meshing. To properly mesh the design, structured mapped meshing on the top face of the geometry was created, breaking up the cells and the spacing areas between them using the mesh sizing as seen in Figure 15. This mapped mesh was then swept through the model, using a distribution of 5, adding 5 layers of elements in each layer of the geometry to ensure the mesh is refined in this direction as seen in Figure 16. The mesh is created with 1-D hex elements.

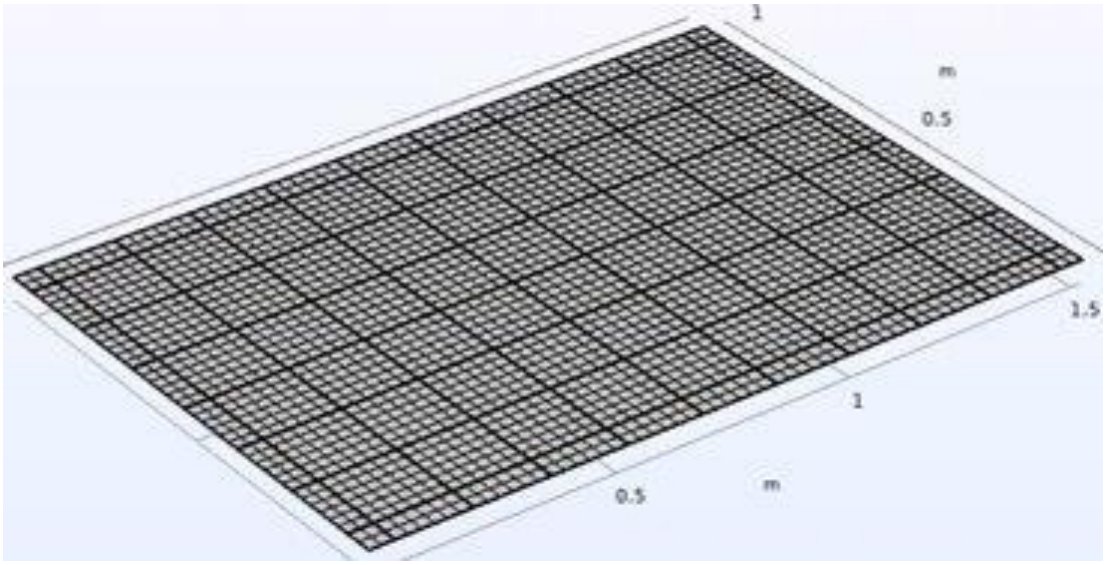

Figure 15: Isometric View of Mesh

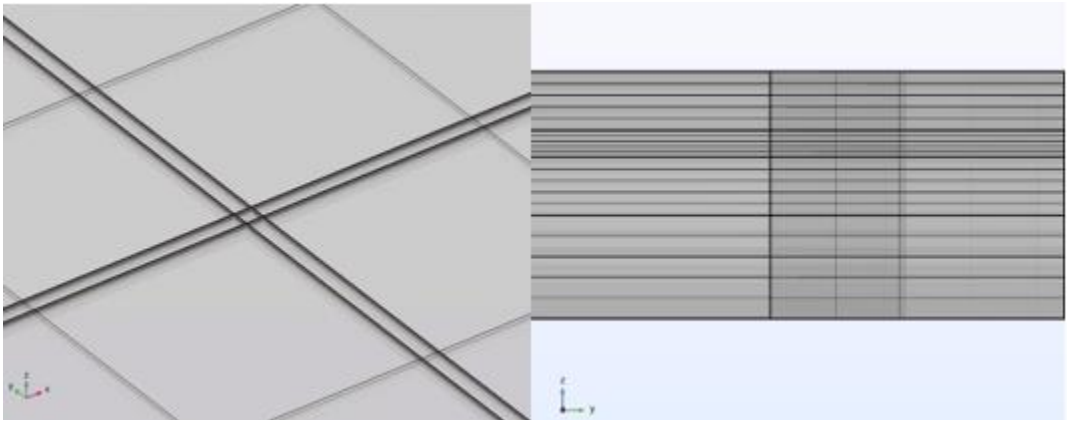

Figure 16: Intersection and Cross-section of Mesh

Meshing is associated with the accuracy of the model, and to guarantee that the mesh brings no extra error to the overall model, a mesh dependency study is done. A mesh dependency study looks at the percent difference in results while doubling the refinement of the mesh and, if these results are within an acceptable range, the original mesh is refined enough to maintain the accuracy desired. On the other side of mesh dependency studies is looking at if the mesh is too fine. Often this is crucial when computation times are extremely long and being able to put less stress on the computer is key to efficiently running simulations. Figure 17 depicts the two meshes, with Mesh 1 being more refined with an element size of 3 cm with a distribution of 5 through each layer. Mesh 2 is less refined with an element size of 5 cm and a distribution of 3 through each layer. Overall, Mesh 1 contains 533615 degrees of freedom and Mesh 2 contains 172175 degrees of freedom.

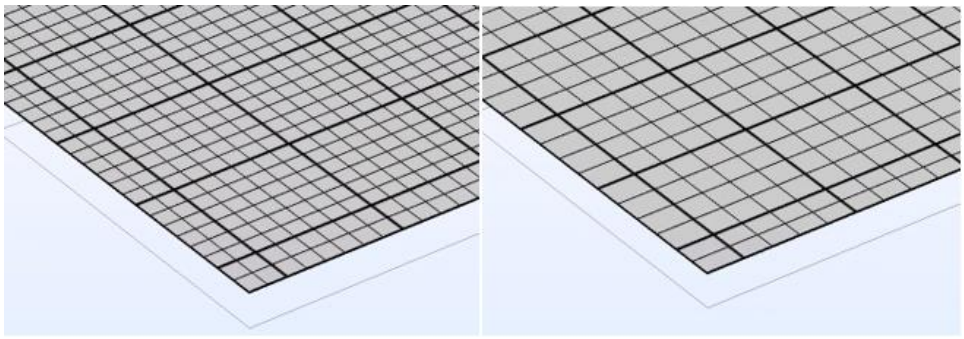

Figure 17: Mesh Refinement Comparison (Mesh 1 left and Mesh 2 right)

The computational time for Mesh 2 increases to 12 mins from 5 mins in the case of Mesh 1. Looking at 3 selected points on the panels, the temperature difference was only an average of 3.1% between Mesh 1 and Mesh 2, which warrants the use of the less refined mesh. Due to concern with simulations with differing environments and the limited computational tax, the more refined Mesh 1 was used.

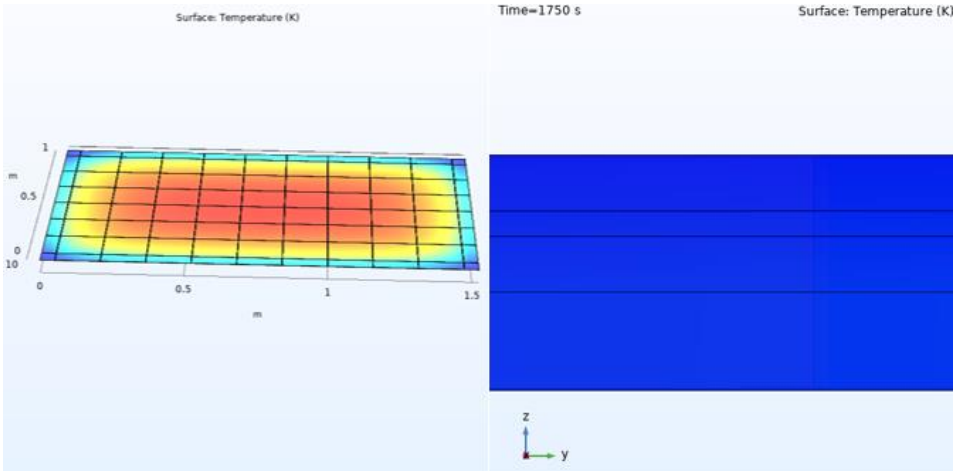

Figure 18: Example Temperature Profile of the Module

Figure 18 shows a typical temperature distribution for a simulation. This simulation was performed using Denver latitude (39.7) and summer season insolation (865 W/m^2) and the city drive cycle as inputs. The simulation was performed on a standard desktop

computer with 32 GB of RAM and was completed in 15 minutes. It is seen that the temperature distribution is symmetrical in this geometry. This is because the heat losses are modeled using averaged coefficients without resolving the surrounding air domain. For all the parametric studies discussed in the next chapter, the volume averaged cell temperatures were extracted and plotted as a function of time.

Chapter 3. Results and Discussion

3.1 Effect of Drive Cycle

To analyze the changes that occurred due to differing types of common drive cycles, data from NREL's Drive Cycle Analysis Tool (NREL, 2021) was used to create a transient velocity versus time plots that could be used as an input in the convective cooling equation for the system. The changes in cooling should result in different drops in efficiency and, as a result, different temperature and power profiles. The drive cycles selected cover the different types of drives a car may experience based on how urban/rural a location may be. The urban drive cycle includes many stops and never sees the speed above 25 mph, and represents the driving seen in the city streets of New York, Los Angeles, and other large cities. The suburban drive cycle covers the drives in lower population cities or more town sized areas, with less frequent stops and slightly higher speeds, around the 35-mph mark. The highway drive cycle represents highway driving as it has very few stops and speeds that are around 50–60 mph. Finally, a stopped drive cycle was used to simulate a parked car in the sunlight, which just maintains a 0 velocity across the time of the simulation representing the worst-case scenario. The simulations for this section were ran using the weather data for Denver in the summer and the cells as mono-Si.

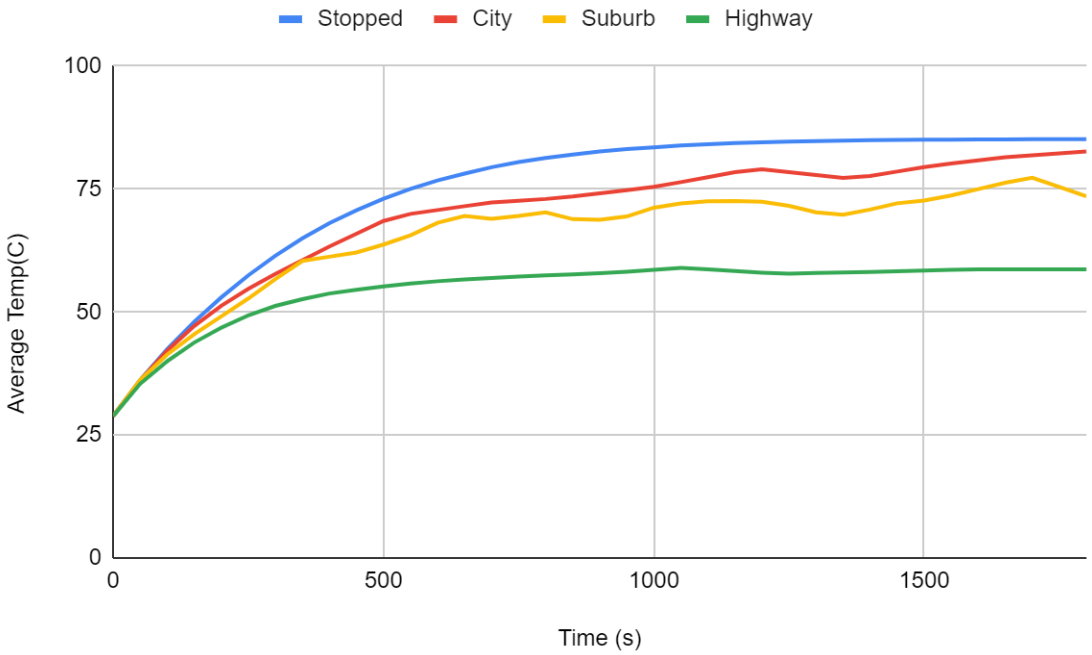

Figure 19: Cell Temperature Comparison of Drive Cycles

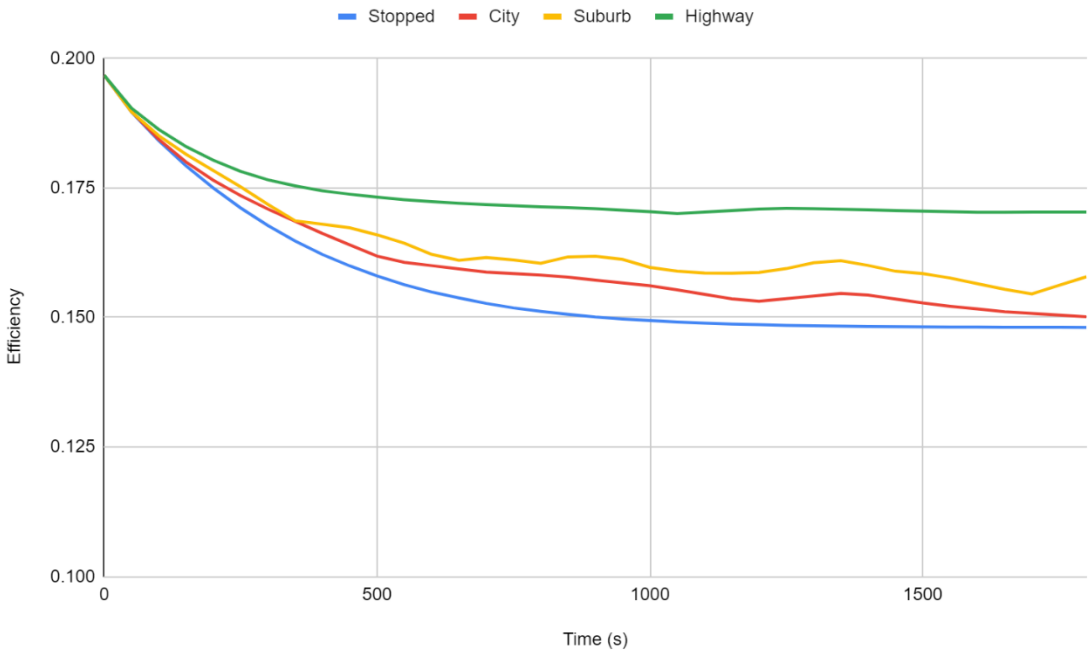

Figure 20: Efficiency Comparison of Drive Cycles

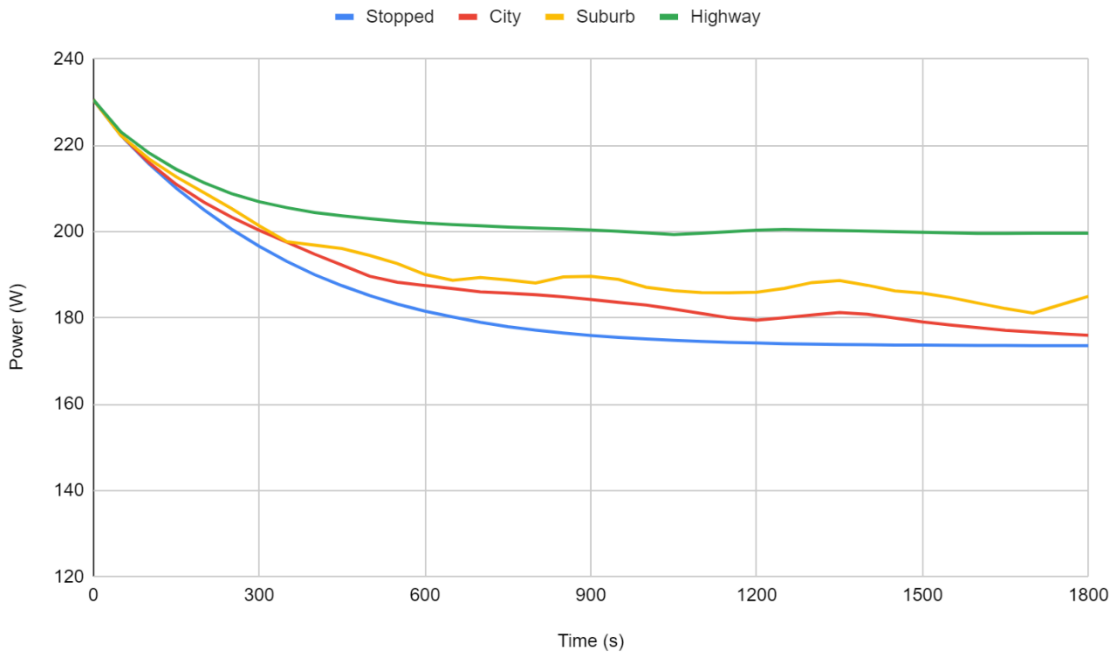

Figure 21: Predicted Power Comparison of Drive Cycles

The results of the drive cycle comparison are the most straight forward since the only aspect of this simulation changing is the input wind speed on the top surface of the module. The constant season and location maintain the rest of the parameters including insolation and ambient temperature, so we see the direct effects of windspeed on the performance of the VIPV module. Since a faster windspeed should produce higher cooling effects thus not inhibiting efficiency, we see the trend that faster drive cycles result in a higher efficiency and power production as displayed in Figure 20 and Figure 21, with a lower cell temperature as seen in Figure 19. This trend supports the idea that VIPV could have a very promising future with applications on shipping trucks and vans that travel at

higher speeds on highways, as the efficiency in this application would be maintained better than a city bus application.

3.2 Effect of Location

Analyzing the effects of different locations, introduces changes in two aspects of the heat transfer problem surrounding VIPV: ambient temperature and insolation. To study the locations, three cities in the United States were chosen with varying latitudes. Miami provides a latitude closer to the equator (25.8) with high year-round temperatures (average highs of 88 F in July and 74 F in January). Also included is Denver as a central latitude (39.7) with lower temperatures (average highs of 92 F in July and 49 F in January) than Miami. Finally, Seattle is used with far lower temperatures (average highs of 73 F in July and 46 F in January) and the farthest latitude (47.6) from the equator. These cities will give an idea the effects of both the ambient temperature and insolation on the temperatures and efficiencies of the cells across the US. Weather data for these cities was gathered using insolation files on Plant Predict (FirstSolar, 2021) that were collected by NREL weather stations.

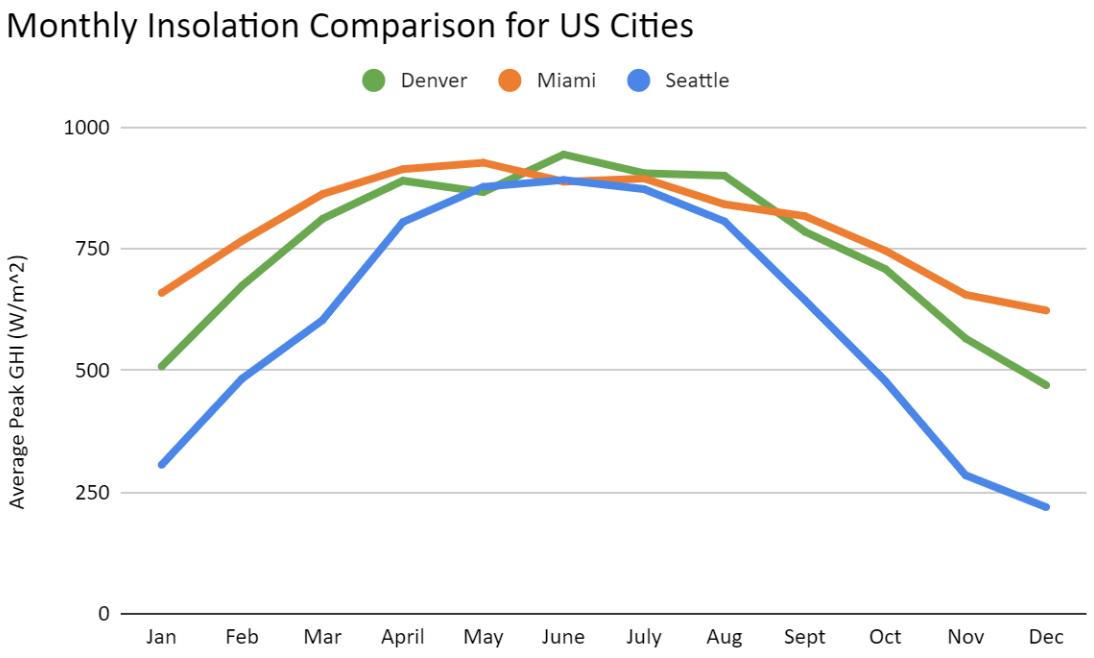

Figure 22: Insolation Values at Peak Hours for Seasons at Selected Locations

In Figure 22, we see the difference in monthly insolation trends and a key thing to note moving forward is the difference in drop off in the winter months for the cities. Miami tends to maintain a much higher insolation while Seattle sees a very steep drop off, which carries over to the performance of the VIPV simulations. The simulations were performed looking at both summer and winter weather data using mono-Si cells and using the city drive cycle.

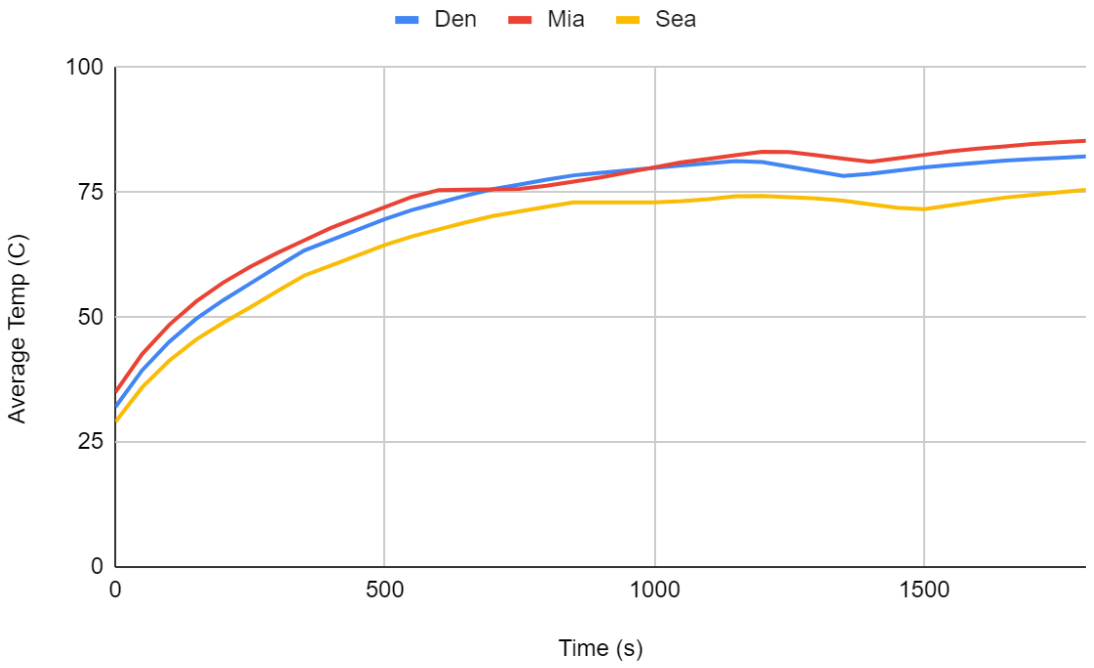

Figure 23: Summer Cell Temperature Comparison of Locations

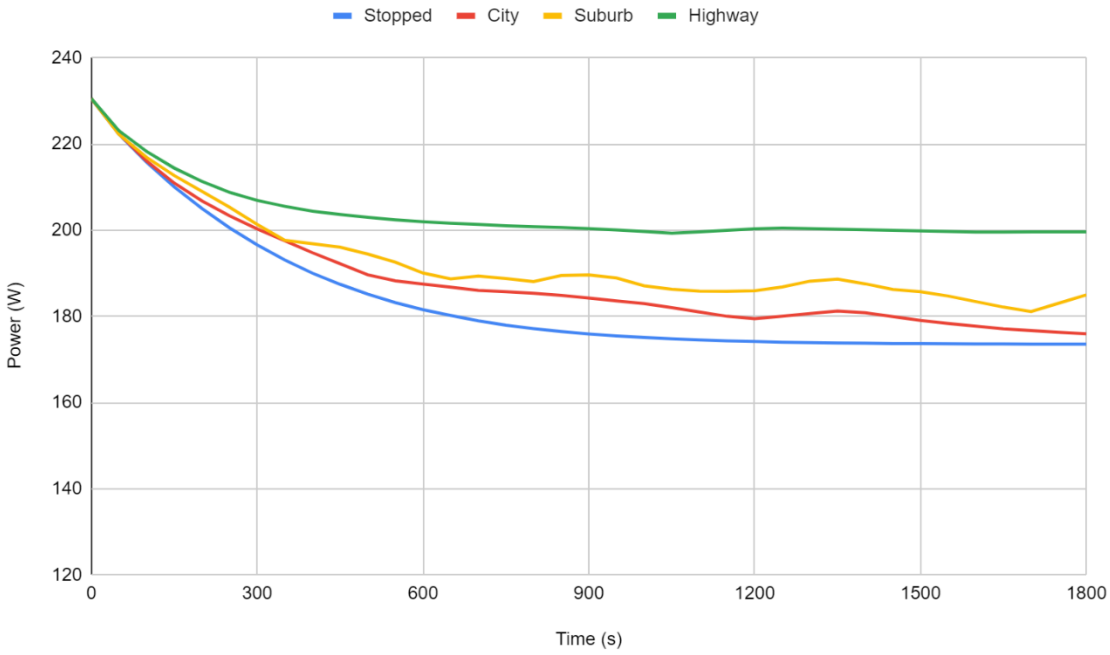

Figure 24: Winter Cell Temperature Comparison of Locations

When comparing Figure 23 and Figure 24, you see drastic differences in the spread of cell temperature data across the locations. In the Winter season, the locations have a variety of nearly 30 degrees C between Miami and Seattle. On the other hand, in Summer the difference between Seattle and Miami is approximately 5 degrees C, showing how the location effects are less apparent in Summer but change the performance from a year-round perspective. These differences are analyzed in more depth in the following Seasonal Comparison section.

3.3 Effect of Season

Similar to the comparison between locations, looking at the seasons within a location bring the different weather trends of each season, adding more ambient temperature and insolation effects due to higher shading in the winters in some locations. This is important to add to analysis as some locations have far more variance in the seasons which can directly affect the outputs in those times. To analyze these effects, GHI data peak times of noon to two was averaged over the course of each season to get an average insolation for these seasons. As introduced before, the weather data used was accessed through Plant Predict (FirstSolar, 2021), collected by NREL weather stations. The simulations were performed with the material set to mono-Si using a city drive cycle.

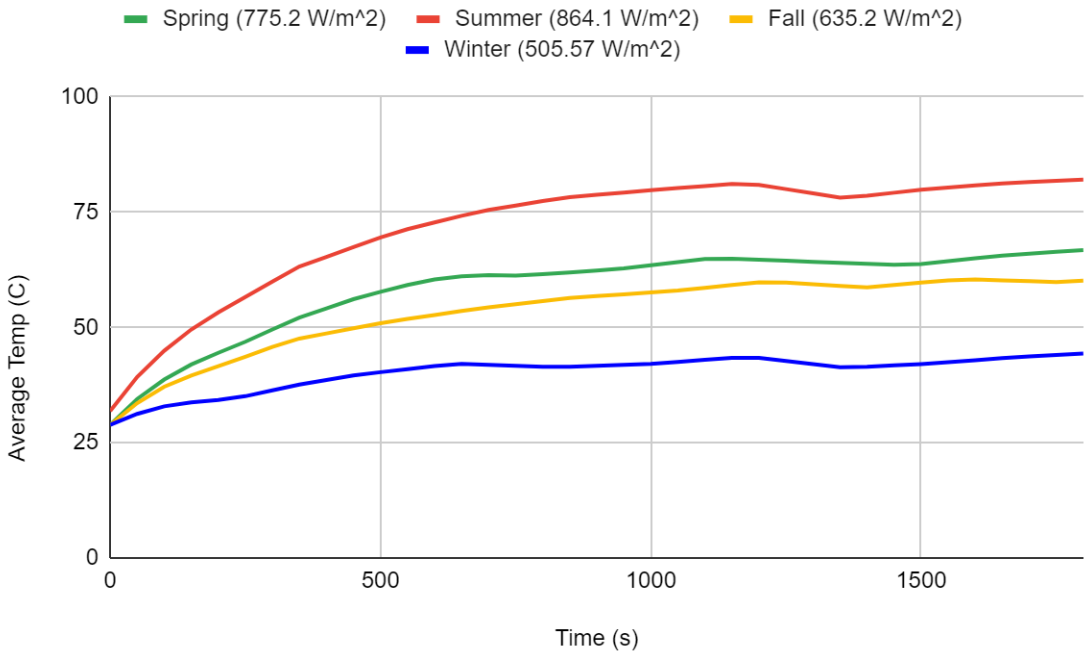

Figure 25: Cell Temperature Comparison of Seasons for Denver

Figure 25 shows the trends of the cell temperatures as the module progresses through a 30-minute drive cycle. All the trends follow what is expected behavior based on ambient temperatures and the changing irradiation. During summer, the module runs the hottest at around 80 degrees Celsius while during winter the module runs the coldest at around 40 degrees Celsius.

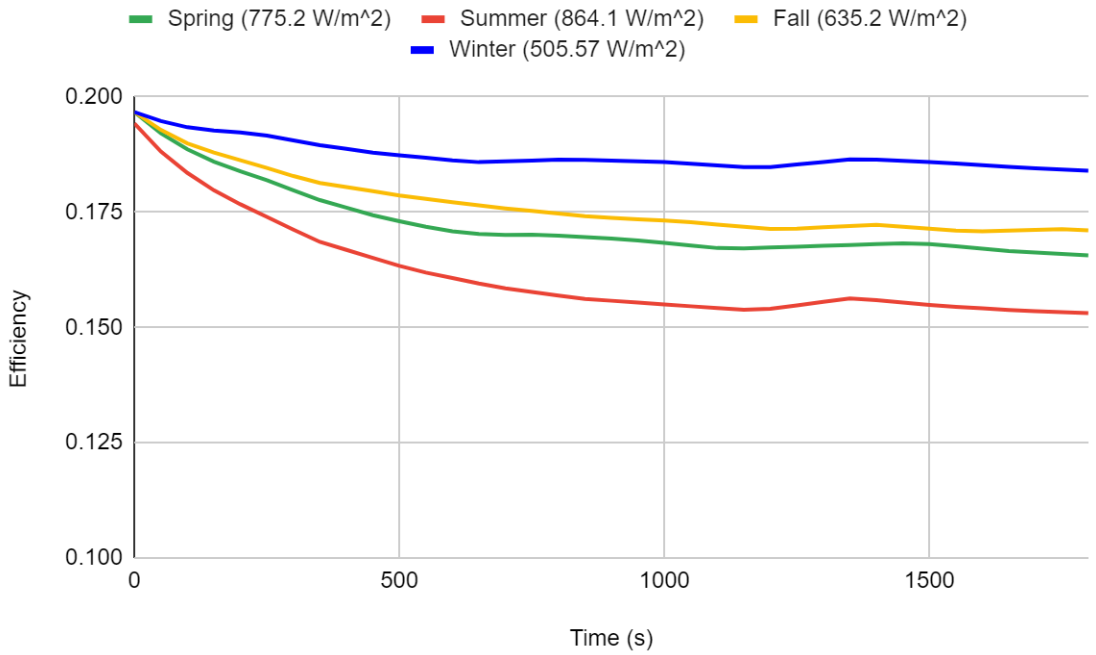

Figure 26: Average Efficiency Comparison of Seasons in Denver

Based on the temperature profiles of the cells we see efficiency trends follow a nearly identical trend but inversed, as the temperatures are inversely related to cell efficiency, so the cooler seasons result in higher cell efficiencies.

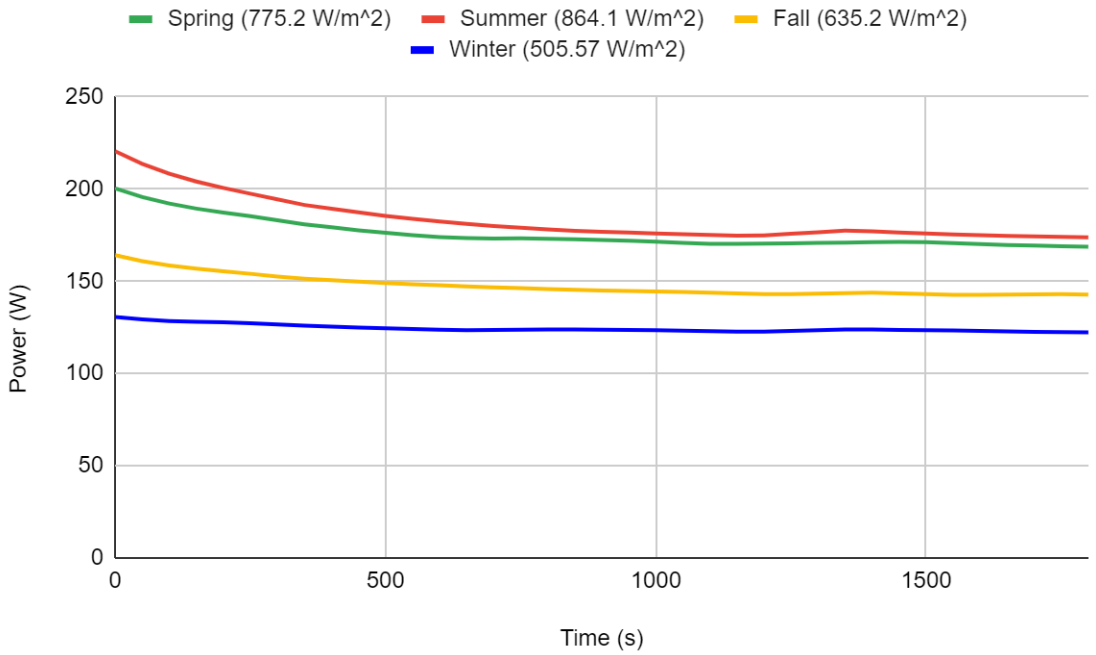

Figure 27: Predicted Power Comparison of Locations in Denver

Considering the differences in efficiency and the variation in seasonal irradiance, the predicted power output based on these values can be generated. The overall trend is similar to that of the efficiency seeing the highest and lowest values as summer and winter respectively. Notably, the spring months we see a massive impact of the effects of ambient temperature, as the irradiation is nearly 100 W/m^2 lower than summer, but by the end of the drive cycle the predicted power is nearly identical to it. This shows the importance of cooling in the performance of VIPV as irradiation alone is not the only factor that needs to be addressed. This also displays the importance of the temperature effects on the material and the impact that temperature has on the efficiency of the cells.

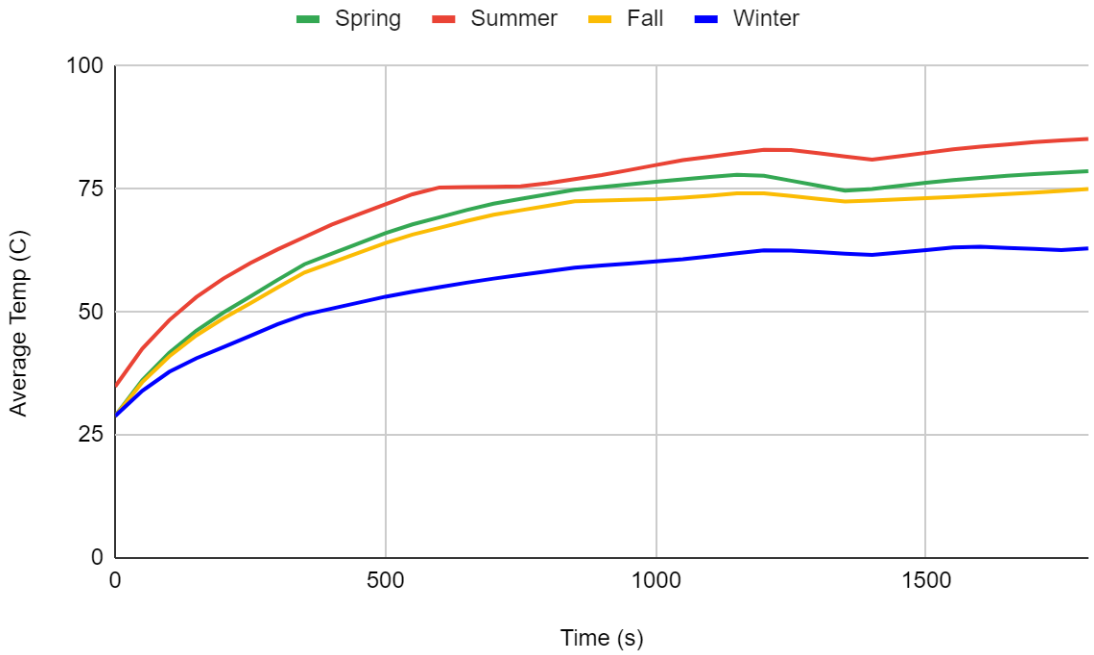

Figure 28: Cell Temperature Comparison for Seasons in Miami

Looking at the effects of seasons on the temperature of the module in Miami, Figure 28 shows the trends all stay much closer when compared to that of Denver's. This is due to the lower variance in both ambient temperature and irradiation experienced in Miami, with higher values year-round that clump the seasons outside of winter rather close together in terms of results.

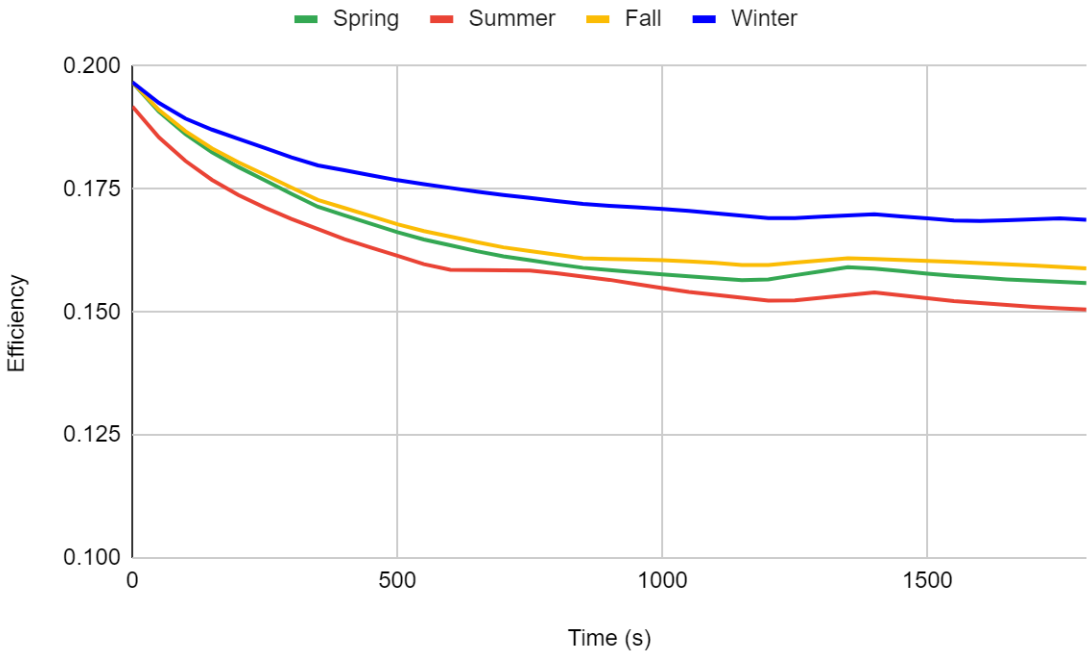

Figure 29: Average Efficiency Comparison of Seasons in Miami

The trend of closer values continues into the efficiency, as it depends indirectly on the temperatures of the module. Compared to the values experienced in Denver, the decreases in efficiency are higher in Miami due to the elevated temperatures.

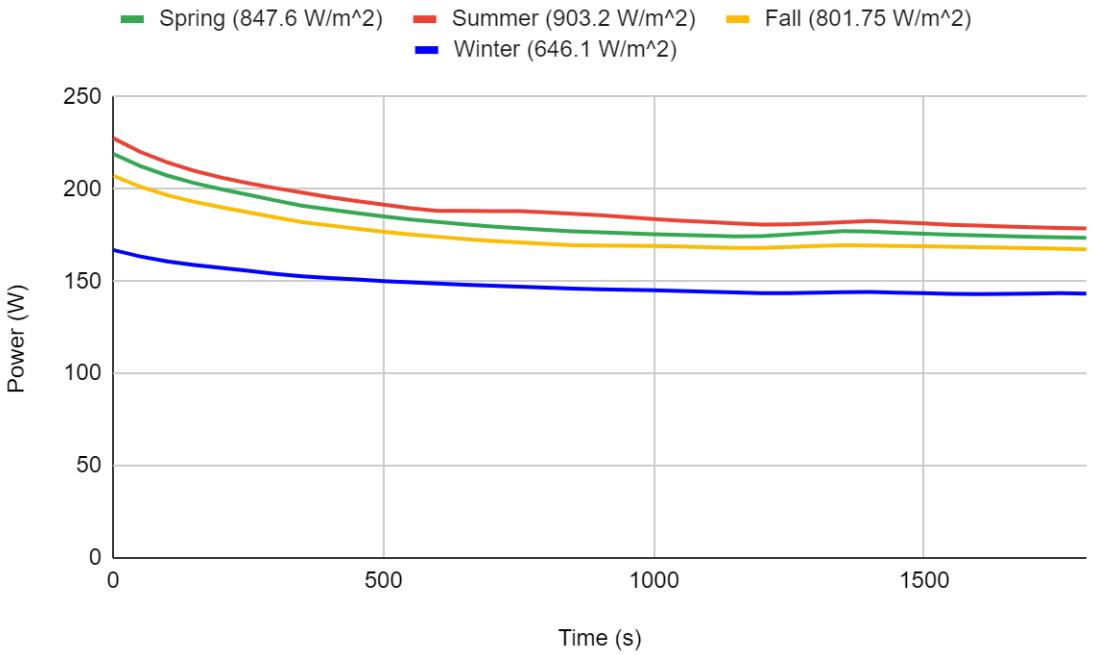

Figure 30: Predicted Power Comparison for Seasons in Miami

Based on the irradiation and the efficiency of the cells, we see a very closely clumped power output from the seasons of Spring, Summer, and Fall. This again shows the importance of cell temperatures in the power output of cells, as maintaining a higher efficiency will provide better power production in lower irradiation months in some cases. Denver's summer power production values are very similar to those found in Miami, but the two cities differ in season consistency, with much more regular temperatures and irradiation in Miami.

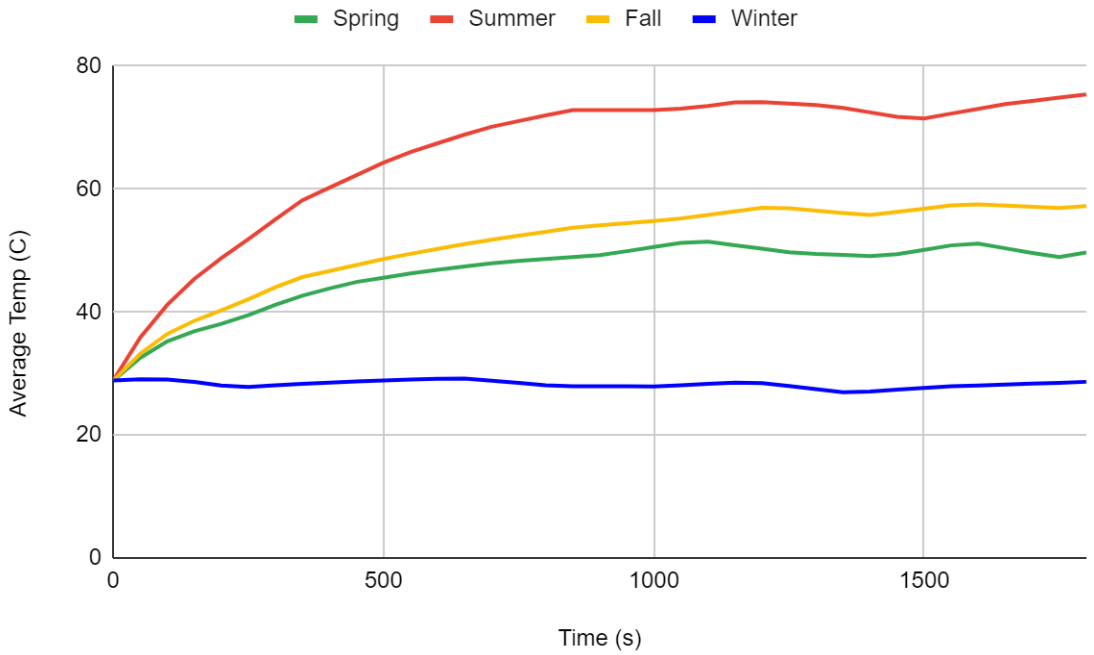

Figure 31: Cell Temperature Comparison for Seasons in Seattle

Figure 31 shows the temperature of the cells in the different seasons at Seattle, showing a much wider distribution due to the highly varying ambient temperatures and irradiations. The cell temperatures in winter remain approximately only 30 degrees Celsius with the summer reaching similar temperatures as the summer in Denver at around 75-80 degrees Celsius.

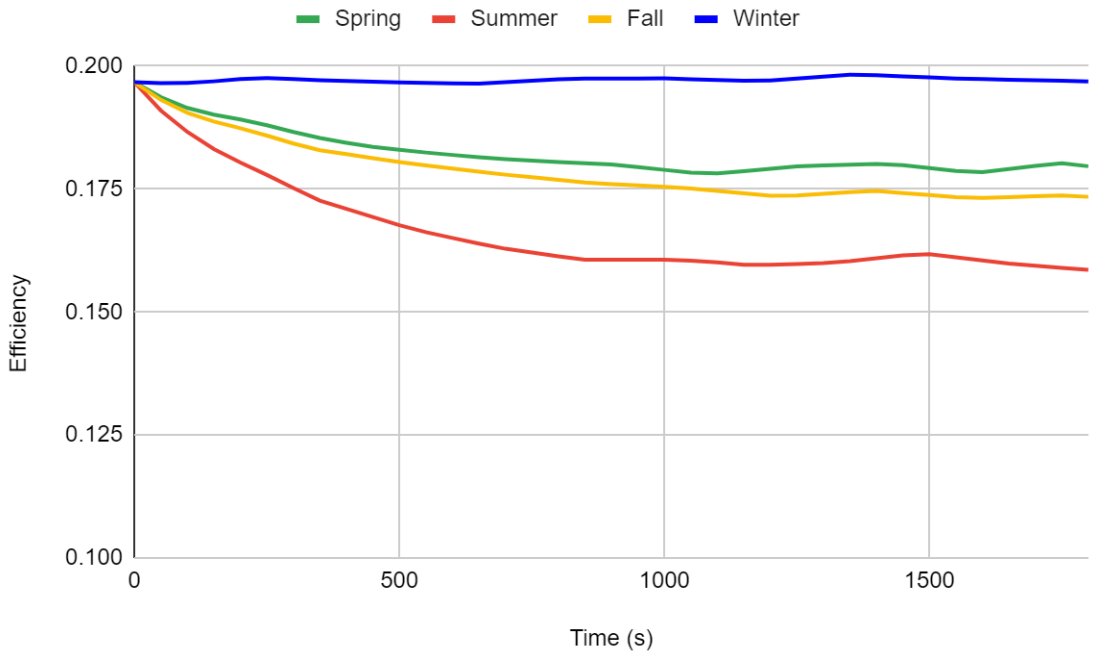

Figure 32: Average Efficiency Comparison for Seasons in Seattle

The widely varying temperature trends are reflected in the efficiency of the cells, as we see a variance of almost 4% between summer and winter seasons. The temperature of the cells in winter are low enough that the efficiency sees even slight increases from the prescribed initial temperature of the module.

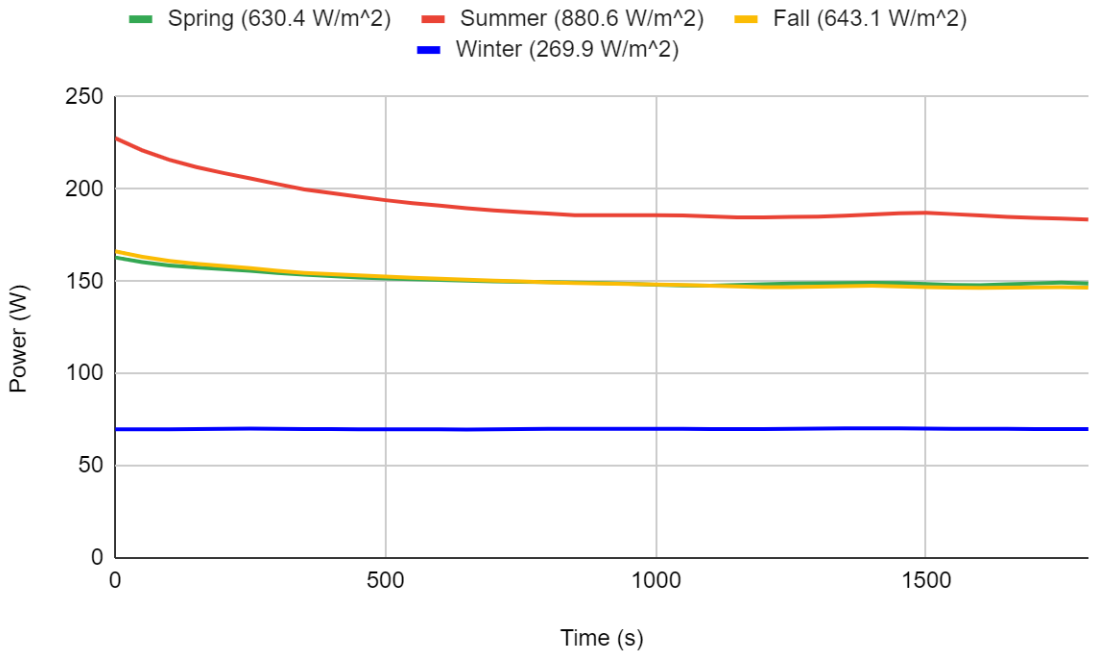

Figure 33: Predicted Power Comparison for Seasons in Seattle

These ranging efficiencies and widely varying values for irradiation contribute to the massive spread in the predicted power outputs of the module, with winter having extremely low values for production. We experience a difference in power production of approximately 100 W with the panel reaching its steady state temperatures in the drive cycle. Seattle's extremely cloudy winters are a great example of the power output of a module in a non-favored PV environment, and although this lower production may not be able to take the brunt of the cars load for driving, it can certainly power many of the auxiliary aspects of the vehicle, like heating and cooling, to ease the load on the battery.

3.4 Effect of PV Material

A massively important aspect of VIPV that must be explored moving forward is the effects of the materials on the temperatures and efficiencies within the module. To maintain simplicity, geometry of the model was unaltered for different packaging materials and rather the different cell materials were varied. In this study, Cadmium Telluride (CdTe) was selected for comparison, as it has a lower temperature coefficient and similar efficiency of 18% when compared to monocrystalline silicon. This suggests CdTe could be more ideal for VIPV applications. CdTe provides a realistic option as it already is competitive in the PV market through companies like First Solar with price per watts around $0.30 for CdTe while the average for mono-Si is around $0.25 (FirstSolar, 2020). Another material investigated was Copper Indium Gallium Selenide (CIGS) as it currently has efficiencies of 17% and has great potential in flexible application as it can be integrated using different substrate materials but is still a less developed material overall. CIGS offers an option with a high potential, as it already has a low temperature coefficient meaning a small effect from the temperature on efficiency while the efficiency can still be improved upon. Finally, Gallium Arsenide (GaAs) was included as it provides an extremely high efficiency at 23% with lower temperature coefficients, but it is a more expensive material that has caught less of a hold on the commercial PV market. Material values were drawn from companies' info sheets (Alta Devices, 2014; FirstSolar, 2020; MiaSole, 2017) on modules in the market to ensure it was not the lone cell efficiencies of lab testing.

The simulations comparing these PV materials were performed with the location set to Miami using insolation and ambient temperature data for summer. The drive cycle

was set to city drive cycle, hoping to see the effects of the temperature coefficients in a higher temperature environment.

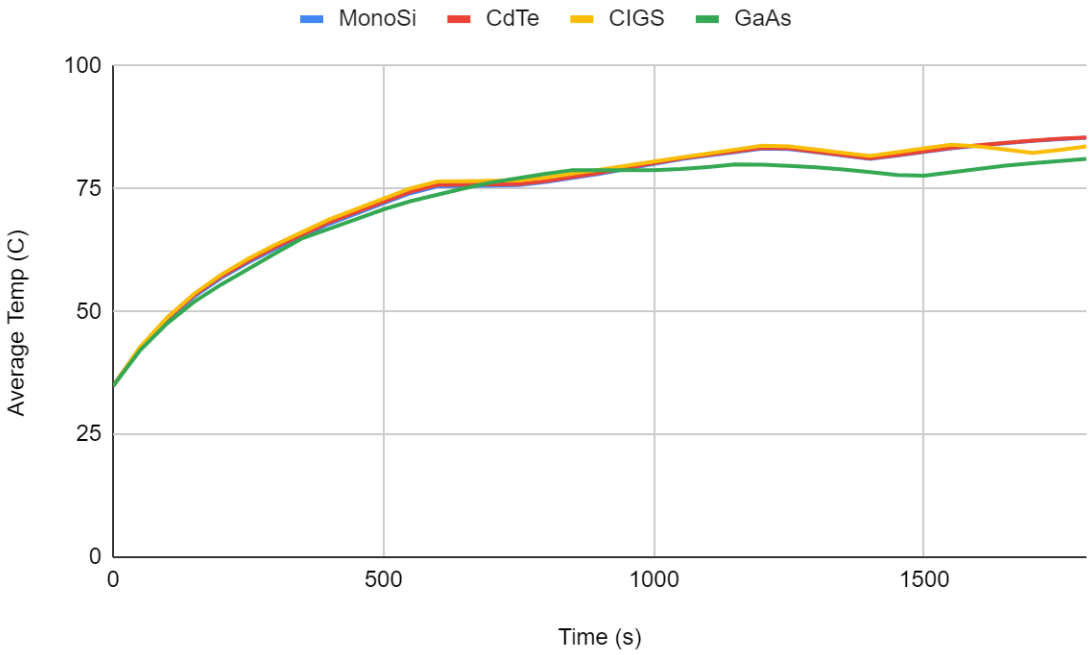

Figure 34: Cell Temperature Comparison for PV Materials

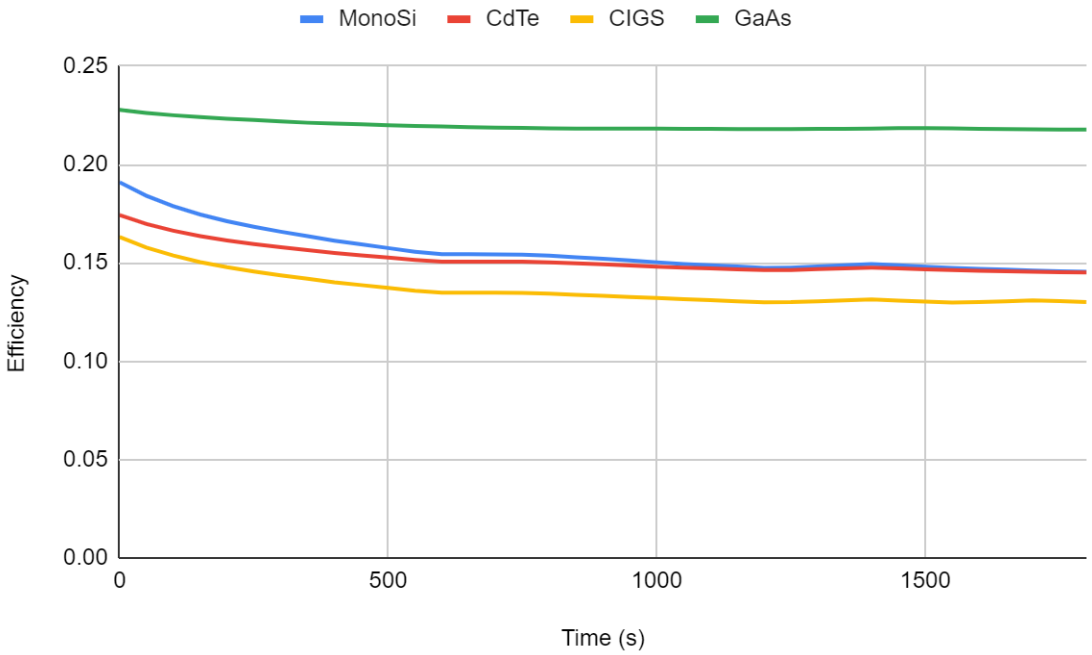

Figure 35: Average Efficiency Comparison for PV Materials

The notable differences in efficiency are clearly on display between these materials, with GaAs leaps and bounds ahead of the rest of the materials. The most notable takeaway from the Figure 35 is the effect of the temperature coefficient between mono-Si and CdTe. Comparing the two we can see that mono-Si has a better initial efficiency than the CdTe, but the temperature coefficient for CdTe is more ideal, and we see a lower effect on the efficiency to the point that the performance of the two is identical by the end of the drive cycle. The power production trend for this simulation directly matches the efficiency trends since there are no changes to drive cycle, insolation, and ambient temperatures in the cells.

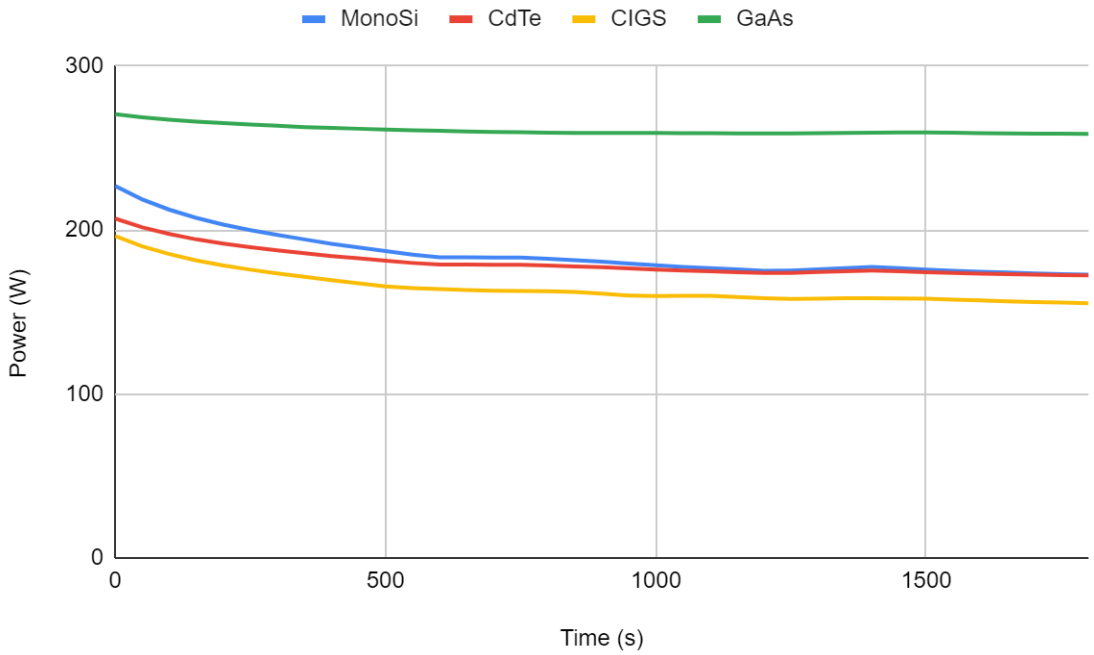

Figure 36: Predicted Power Comparison for PV Materials

3.5 Thermal Stresses

To analyze the effects of temperatures in the model on stresses, the equivalent stresses were analyzed in the worst-case scenario, Miami in the summer. The model structurally is fixed using boundary conditions on the bottom face of the module as well as the edges, which replicates how the model would be fixed in a real scenario. This limits the expansion of the model in the XY direction and causes stresses due to that. An equivalent von Mises stress distribution within the panel is shown in Figure 37, with maximum values nearing $6x10^7$ Pa. For comparison, the ultimate tensile strength of monocrystalline silicon is $7x10^9$ Pa, so the maximum stress is two orders of magnitude lower than this. While the maximum static stress may not be concerning, the cycling of these stresses is what can cause lasting damage to the panels.

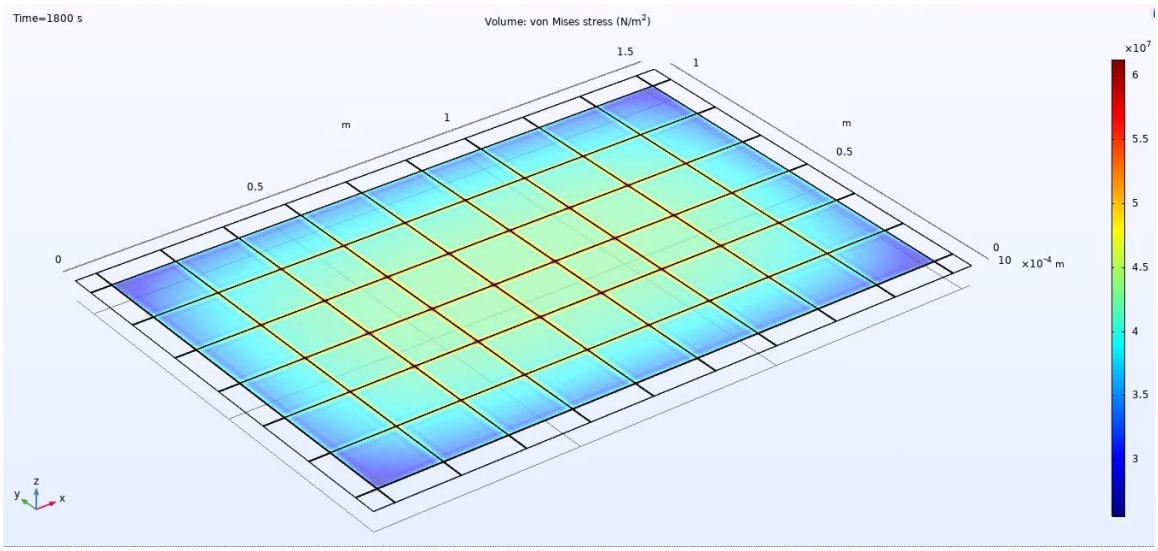

Figure 37: Isometric View of Stress Contour on the Module

Further analysis must be carried out for VIPV modules to ensure the thermal effects do not cause increased degradation of the panels. Trends are already seen in normal PV applications that the PV module output is inhibited by the hotter environments and they experience a higher average decrease in efficiency every subsequent year. With the excessive temperatures in VIPV the delamination of the materials must be analyzed as the high temperatures may be detrimental. To understand the extent of these effects, the possible temperatures of VIPV along with the design for the modules will need to experience extensive iterative testing to quantify these degradation losses. Although degradation is a key in the design of VIPV modules, studying degradation mechanisms and its effects are outside the scope of this study. The thermal work performed in this study will provide a framework for future work in exploring VIPV reliability and the challenges associated with it.

Chapter 4. Conclusion

4.1 Summary

On the forefront of a shift to EVs and alternative sources of power, advancements in EVs are key to the ease and speed of the transition. One major technological opportunity is the use of vehicle integrated photovoltaics in EVs to increase the range and overall efficiency of the vehicles, getting more power from a direct clean source. Although the concept of VIPV appears great at first glance, many challenges arise with the altered aspects of the PV system. To better understand the necessary steps and the current viability of PV technology in a VIPV application, gauging the temperatures and the predicted effects on other aspects of the modules is important. This study created a model that predicts temperatures of this application with varying parameters and provides a sense of the temperatures captured in this setting.

Numerical modeling the system entails first fully understanding the heat transfer occurring within the model and subsequently making acceptable assumptions surrounding these equations. In this case, the system scope was framed to only look at the heat stored, lost, and gained from the system and the effects on the temperatures within the cells. Geometry of a module was replicated in COMSOL and the boundary conditions of the heat transfer problem were applied. Using inputs associated with various parameters including location, season, and drive cycle, the system was analyzed and effects on the efficiency and predicted power production were compared. Looking at the seasonal effects, we see temperatures in the panel upwards of 80 degrees Celsius in the summer. Winters see lower temperature and production values across locations, but we see the primary difference in

the locational effects in the winter, as differing latitudes will experience far colder winters with less sunlight exposure and hours in the day. Drive cycles directly affect the cooling of the module, with faster drive cycles decreasing the temperature as much as 20 degrees Celsius from a standstill VIPV module in the same environment. We also see that the drop in efficiency due to higher ambient temperatures has enough of an effect that spring has rather similar power production with lower insolation values when compared to summer in Denver.

4.2 Future Work and Suggestions

Based on the progress made with this study, there are many more factors of VIPV that need to be analyzed moving forward. The recommended next steps for this project or area of research moving forward are listed below:

- Including curvature of roof in modeled geometry (or correction factor) – correction for curvature is important because this affects the insolation reaching the solar cells as well as shading on the module.
- Testing different cell layout configurations and types (shingled, thin film) – shingled allows you to increase packing density which can help with higher power system with given area, while thin film adds flexibility for curved surfaces and low temperature coefficients.
- Including weights of different PV materials and packaging methods – specific weights of PV materials are an extremely important aspect moving forward as the weight directly adds load to the vehicle so finding options with high specific weights is crucial.

- Analyze the structural effects due to delamination at the higher temperatures of VIPV – structural integrity and reliability is key in PV applications because often you are making a large up-front payment and trusting the design to last long enough to see value added from the product. Quantifying the reliability centered effects of the high temperatures is important in the design process of VIPV.
- Applying to Building integrated photovoltaics (BIPV) – this study sets a lot of groundwork down for similar PV applications to VIPV such as BIPV. The two applications have extremely similar heat transfer situations with slightly different cooling aspects on the convective front.

Bibliography

Alta Devices. (2014). *Single Cell Alta Devices produces the highest performance single junction solar cells available on the market* . 94085.

Arora, P. (2016). Multiphysics simulation of PV modules. *MSc Thesis. Instituto Superior Técnico*, *October*, 82.

Bergman, T. L., Lavine, A. S., Incropera, F. P., & DeWitt, D. P. (2015). Fundamentals of heat and mass transfer, 2011. In *USA: John Wiley & Sons. ISBN* (Vol. 13).

Chander, S., Purohit, A., Sharma, A., Arvind, Nehra, S. P., & Dhaka, M. S. (2015). A study on photovoltaic parameters of mono-crystalline silicon solar cell with cell temperature. *Energy Reports*, *1*. https://doi.org/10.1016/j.egyr.2015.03.004

FirstSolar. (2020). *Advanced Thin Film Solar Technology*. 1–2.

FirstSolar. (2021). *Plant Predict*. https://ui.plantpredict.com/weather-library/

Fraunhofer. (2021). *Vehicle-Integrated Photovoltaics*.

Gersdorf, T., Hertzke, P., Schaufuss, P., & Schenk, S. (2020). McKinsey Electric Vehicle Index: Europe Cushions a Global Plunge in EV Sales. *McKinsey & Company*, *July*(July).

Green, M. A. (2019). How Did Solar Cells Get So Cheap? In *Joule* (Vol. 3, Issue 3). https://doi.org/10.1016/j.joule.2019.02.010

Hanergy. (2021). *Fully Solar-powered Cars of*. http://en.hanergythinfilmpower.com/index.php?m=content&c=index&a=lists&catid=165

Hyundai. (2021). *SONATA Hybrid 2021*.

Lee, Y., & Tay, A. A. O. (2012a). Finite element thermal analysis of a solar photovoltaic module. *Energy Procedia*, *15*(2011), 413–420. https://doi.org/10.1016/j.egypro.2012.02.050

Lee, Y., & Tay, A. A. O. (2012b). Finite element thermal analysis of a solar photovoltaic module. *Energy Procedia*, *15*. https://doi.org/10.1016/j.egypro.2012.02.050

Lightyear. (2021). *Drive for months without charging . Clean and*. https://lightyear.one/

MiaSole. (2017). *FLEX SERIES -01W CIGS Flexible Modules : High Power Density in a Flexible Form Factor*. 1–2.

Nižetić, S., Grubišić- Čabo, F., Marinić-Kragić, I., & Papadopoulos, A. M. (2016). Experimental and numerical investigation of a backside convective cooling mechanism on photovoltaic panels. *Energy*, *111*, 211–225. https://doi.org/10.1016/j.energy.2016.05.103

NREL. (2021). *DriveCAT : Drive Cycle Analysis Tool Select a Drive Cycle How to Cite the Data*. https://www.nrel.gov/transportation/drive-cycle-tool/

Nyanor, P. (2015). 3D Finite Element Method Modeling and Simulation of the Temperature of Crystalline Photovoltaic Module. *International Journal of Research in Engineering and Technology*, *04*(09), 378–384. https://doi.org/10.15623/ijret.2015.0409070

Reese, M. O., Glynn, S., Kempe, M. D., McGott, D. L., Dabney, M. S., Barnes, T. M., Booth, S., Feldman, D., & Haegel, N. M. (2018). Increasing markets and decreasing package weight for high-specific-power photovoltaics. *Nature Energy*, *3*(11), 1002–1012. https://doi.org/10.1038/s41560-018-0258-1

Siddiqui, M. U., & Arif, A. F. M. (2013). Electrical, thermal and structural performance of a cooled PV module: Transient analysis using a multiphysics model. *Applied Energy*, *112*. https://doi.org/10.1016/j.apenergy.2013.06.030

Sono Motors. (2016). *Powered by the Sun*. Sono Motors. https://doi.org/10.2505/4/tst16_083_03_25

Toyota Motor Corporation. (2019). NEDO, Sharp, and Toyota to Begin Public Road Trials of Electrified Vehicles Equipped with High-efficiency Solar Batteries _ Corporate _ Global Newsroom _ Toyota Motor Corporation Official Global Website. *NEDO, Sharp, and Toyota to Begin Public Road Trials of Electrified Vehicles Equipped with High-Efficiency Solar Batteries _ Corporate _ Global Newsroom _ Toyota Motor Corporation Official Global Website*, *5*, 1–6.

Usama Siddiqui, M., Arif, A. F. M., Kelley, L., & Dubowsky, S. (2012). Three-dimensional thermal modeling of a photovoltaic module under varying conditions. *Solar Energy*, *86*(9). https://doi.org/10.1016/j.solener.2012.05.034